THESIS FOR THE DEGREE OF DOCTOR OF PHILOSOPHY

Kinetic modelling of runaways in plasmas

OLA EMBRÉUS

Department of Physics
CHALMERS UNIVERSITY OF TECHNOLOGY
Göteborg, Sweden, 2019

Kinetic modelling of runaways in plasmas
OLA EMBRÉUS
ISBN 978-91-7597-840-6

Doktorsavhandlingar vid Chalmers tekniska högskola
Ny serie nr 4521
ISSN 0346-718X

Department of Physics
Chalmers University of Technology
SE-412 96 Göteborg
Sweden
Tel: +46 (0) 31 772 1000

Cover: Momentum-space contours of the electron distribution function on a logarithmic scale. Steady-state solutions of the spatially homogeneous kinetic equation in the presence of a constant electric field, collisions and bremsstrahlung losses.

Printed in Sweden by
Reproservice
Chalmers Tekniska Högskola
Göteborg, Sweden, 2018

Kinetic modelling of runaways in plasmas

Ola Embréus
Department of Physics
Chalmers University of Technology

Abstract

The phenomenon of runaway occurs in plasmas in the presence of a strong electric field, when the accelerating force overcomes the collisional friction acting on the charged particles moving through the plasma. Runaway is observed in both laboratory and space plasmas, and is of great importance in fusion-energy research, where the energetic runaway electrons can damage the plasma-facing components of fusion reactors.

In this thesis, we present a series of papers which investigate various aspects of runaway dynamics. We advance the kinetic description of electron runaway by deriving and analyzing a fully conservative large-angle collision operator suitable for studying runaway dynamics, and explore its impact on runaway generation and decay. We also present a generalization of the Landau-Fokker-Planck equation to describe screening effects in partially ionized plasmas, providing improved capability of modelling the effect of runaway mitigation schemes in fusion devices.

The emission of synchrotron and bremsstrahlung radiation are important energy-loss mechanisms for relativistic runaway electrons, and they also provide essential diagnostic tools. We demonstrate the need for a stochastic description in order to accurately describe the effect of bremsstrahlung radiation losses on the electron motion. Synchrotron radiation is often emitted at visible and infrared wavelengths in tokamaks, allowing the emission to be readily observed. We have developed a synthetic radiation diagnostic tool, SOFT, which provides new insight into how features of the runaway distribution can affect the observed emission patterns.

Finally, we have investigated the runaway dynamics of ions and of positrons which are generated during runaway. The runaway description in these cases differs from regular electron runaway due to the high mass of the ions, and the fact that positrons are created with a large momentum antiparallel to their direction of acceleration.

Keywords: plasma, runaway, Boltzmann equation, Fokker-Planck equation, bremsstrahlung, synchrotron radiation, tokamak, positrons

Publications

This thesis is based on the work contained in the following papers, which can be found appended at the end of the thesis:

A O. Embréus, A. Stahl and T. Fülöp,
On the relativistic large-angle electron collision operator for runaway avalanches in plasmas,
Journal of Plasma Physics **84**, 905840102 (2018).
https://doi.org/10.1017/S002237781700099X

B O. Embréus, A. Stahl and T. Fülöp,
Effect of bremsstrahlung radiation emission on fast electrons in plasmas,
New Journal of Physics **18**, 093023 (2016).
https://doi.org/10.1088/1367-2630/18/9/093023

C O. Embréus, L. Hesslow, M. Hoppe, G. Papp, K. Richards and T. Fülöp,
Dynamics of positrons during relativistic electron runaway,
Journal of Plasma Physics **84**, 905840506 (2018).
https://doi.org/10.1017/S0022377818001010

D O. Embréus, S. Newton, A. Stahl, E. Hirvijoki and T. Fülöp,
Numerical calculation of ion runaway distributions,
Physics of Plasmas **22**, 052122 (2015).
https://doi.org/10.1063/1.4921661

E L. Hesslow, O. Embréus, M. Hoppe, T. C. DuBois, G. Papp, M. Rahm and T. Fülöp,
Generalized collision operator for fast electrons interacting with partially ionized impurities,
Journal of Plasma Physics **84**, 905840605 (2018).
https://doi.org/10.1017/S0022377818001113

F M. Hoppe, O. Embréus, R. A. Tinguely, R. S. Granetz, A. Stahl and T. Fülöp,
SOFT: A synthetic synchrotron diagnostic for runaway electrons,
Nuclear Fusion **58**, 026032 (2018).
https://doi.org/10.1088/1741-4326/aa9abb

Statement of contribution

Paper A: I derived the new theory (most notably equations (2.23-24)) and implemented it in the numerical kinetic solver. I performed all simulations, produced all figures, and prepared the draft of sections 2 and 3. I contributed with finalizing the manuscript together with the co-authors.

Paper B: I was responsible for all calculations as well as their numerical implementation, I performed the simulations and prepared all figures. I wrote the draft of the second and third sections, as well as contributed to the preparation of the final version of the manuscript.

Paper C: I carried out all the calculations and derivations in the paper, participated in the numerical implementation of the theory and produced the results shown in figures 1, 2 and 4. I prepared the entire draft of the manuscript, exluding parts of the introduction and conclusions, and I was involved in finalising the text for publication.

Paper D: I was responsible for all simulations and calculations, as well as developed the CODION tool. I wrote all parts of the text presenting new calculations or results, and produced all the figures.

Paper E: Throughout the project I was involved with exploring and developing ideas and calculations for the paper. In particular, I was mainly responsible for the calculations presented in section 4 and appendix B. I assisted in finalizing the manuscript for publication.

Paper F: I was involved with the design of the SOFT tool, and derived the theory presented in section 2.1 and 2.3. I contributed with analysis and interpretation to all results presented. I assisted in finalizing the manuscript for publication.

Related publications, not included in the thesis

G A. Stahl, E. Hirvijoki, J. Decker, O. Embréus and T. Fülöp,
Effective critical electric field for runaway electron generation,
Physical Review Letters **114**, 115002 (2015).
http://doi.org/10.1103/PhysRevLett.114.115002

H E. Hirvijoki, I. Pusztai, J. Decker, O. Embréus, A. Stahl and T. Fülöp,
Radiation reaction induced non-monotonic features in runaway electron distributions,
Journal of Plasma Physics **81**, 475810502 (2015).
http://doi.org/10.1017/S0022377815000513

I E. Hirvijoki, J. Decker, A. Brizard and O. Embréus,
Guiding-center transformation of the Abraham-Lorentz-Dirac radiation reaction force,
Journal of Plasma Physics **81**, 475810504 (2015).
http://doi.org/10.1017/S0022377815000744

J E. Hirvijoki, J. Candy, E. Belli and O. Embréus,
The Gaussian Radial Basis Function method for plasma kinetic theory,
Physics Letters A **379**, 2735 (2015).
https://doi.org/10.1016/j.physleta.2015.08.010

K J. Decker, E. Hirvijoki, O. Embréus, Y. Peysson, A. Stahl, I. Pusztai and T. Fülöp,
Numerical characterization of bump formation in the runaway electron tail,
Plasma Physics and Controlled Fusion **58**, 025016 (2015).
http://doi.org/10.1088/0741-3335/58/2/025016

L A. Stahl, O. Embréus, G. Papp, M. Landreman and T. Fülöp,
Kinetic modelling of runaway electrons in dynamic scenarios,
Nuclear Fusion **56**, 112009 (2016).
http://doi.org/10.1088/0029-5515/56/11/112009

M A. Stahl, O. Embréus, M. Landreman, G. Papp and T. Fülöp,
Runaway-electron formation and electron slide-away in an ITER post-disruption scenario,
Journal of Physics: Conference Series **775**, 012013 (2016).
http://doi.org/10.1088/1742-6596/775/1/012013

N A. Stahl, M. Landreman, O. Embréus and T. Fülöp,
NORSE: A solver for the relativistic non-linear Fokker-Planck equation for electrons in a homogeneous plasma,
Computer Physics Communications **212**, 269 (2017).
https://doi.org/10.1016/j.cpc.2016.10.024

O L. Hesslow, O. Embréus, A. Stahl, T. C. DuBois, G. Papp, S. L. Newton and T. Fülöp,
Effect of partially screened nuclei on fast-electron dynamics,
Physical Review Letters **118**, 255001 (2017).
https://doi.org/10.1103/PhysRevLett.118.255001

P M. Hoppe, O. Embréus, C. Paz-Soldan, R. A. Moyer and T. Fülöp,
Interpretation of runaway electron synchrotron and bremsstrahlung images,
Nuclear Fusion **58**, 082001 (2018).
https://doi.org/10.1088/1741-4326/aaae15

Q R. A. Tinguely, R. S. Granetz, M. Hoppe and O. Embréus,
Measurements of runaway electron synchrotron spectra at high magnetic fields in Alcator C-Mod,
Nuclear Fusion **58**, 076019 (2018).
https://doi.org/10.1088/1741-4326/aac444

R L. Hesslow, O. Embréus, G. J. Wilkie, G. Papp and T. Fülöp,
Effect of partially ionized impurities and radiation on the effective critical electric field for runaway generation,
Plasma Physics and Controlled Fusion **60**, 074010 (2018).
https://doi.org/10.1088/1361-6587/aac33e

S R. A. Tinguely, R. S. Granetz, M. Hoppe and O. Embréus,
Spatiotemporal evolution of runaway electrons from synchrotron images in Alcator C-Mod,
Plasma Physics and Controlled Fusion **60**, 124001 (2018).
https://doi.org/10.1088/1361-6587/aae6ba

Conference contributions

T O. Embréus, S. Newton, A. Stahl, E. Hirvijoki and T. Fülöp,
Numerical calculation of ion runaway distributions,
Proceedings of 42nd EPS Conference on Plasma Physics, Lisbon, P1.401 (2015).
http://ocs.ciemat.es/EPS2015PAP/pdf/P1.401.pdf

U O. Embréus, A. Stahl and T. Fülöp,
Effect of bremsstrahlung emission on fast electrons in plasmas,
Proceedings of 43rd EPS Conference on Plasma Physics, Prague, O2.402 (2016).
http://ocs.ciemat.es/EPS2016PAP/pdf/O2.402.pdf

V L. Hesslow, O. Embréus, G. Wilkie, T. C. DuBois, G. Papp and T. Fülöp,
Fast-electron dynamics in the presence of weakly ionized impurities,
Proceedings of 44th EPS Conference on Plasma Physics, Prague, O4.118 (2017).
http://ocs.ciemat.es/EPS2017PAP/pdf/O4.118.pdf

W A. Stahl, O. Embréus, G. Wilkie, M. Landreman, G. Papp and T. Fülöp,
Self-consistent nonlinear kinetic modeling of runaway-electron dynamics,
Proceedings of 44th EPS Conference on Plasma Physics, Prague, P2.150 (2017).
http://ocs.ciemat.es/EPS2017PAP/pdf/P2.150.pdf

X O. Embréus, A. Stahl and T. Fülöp,
Effect of bremsstrahlung emission on fast electrons in plasmas,
Proceedings of 44th EPS Conference on Plasma Physics, Prague, O2.402 (2017).
http://ocs.ciemat.es/EPS2016PAP/pdf/O2.402.pdf

Y M. Hoppe, O. Embréus, P. Svensson, L. Unnerfelt and T. Fülöp,
Simulations of bremsstrahlung and synchrotron radiation from runaway electrons,
Proceedings of 45th EPS Conference on Plasma Physics, Prague, O5.J603 (2018).
http://ocs.ciemat.es/EPS2018PAP/pdf/O5.J603.pdf

Z O. Embréus, K. Richards, G. Papp, L. Hesslow, M. Hoppe and T. Fülöp,
Dynamics of positrons during relativistic electron runaway,
Proceedings of 45th EPS Conference on Plasma Physics, Prague, P5.4011 (2018).
`http://ocs.ciemat.es/EPS2018PAP/pdf/P5.4011.pdf`

Acknowledgements

I would first like to express my gratitude towards my supervisor Tünde Fülöp – who has mostly been patient with me, against all odds – for providing such a creative work environment and for allowing me into the runaway family. Thanks for always having me pursue the ideas that I have felt the most excited about.

I would like to thank my assistant supervisors Håkan Smith, for his hospitality during my visit to Greifswald, and to Geri Papp, for the lovely email physics conversations, his meticulous attention to detail and for all of our delightful interactions over the years.

Also thanks to Sarah Newton, for showing me the ropes in plasma physics and for the good times in Oxford during my visit. Additionally, I would like to direct my gratitude towards Eero Hivijoki and Joan Decker, who have been there since the start and have inspired me ever since.

Thanks to the entire Chalmers Plasma Theory family, who made this work a pure joy. In particular to Linnea Hesslow, for always striving for perfection, for always challenging my beliefs and for the countless discussions of the intricacies of runaway theory; and to Mathias Hoppe, for the thrilling roller-coaster ride of SOFT development. You have both provided some of my most cherished memories from this time.

Finally, to Brita and Frasse, for all the encouragement and love, and for keeping me reminded of what I do this for.

Ola Embréus, Göteborg, Dec 13, 2018

Contents

Chapter 1

Introduction

A plasma is an ionized gas, sufficiently hot that the electrons have detached from the atoms that carried them. Because it consists of free charges, rather than neutral atoms, a plasma behaves differently to the familiar gases and fluids encountered in everyday life. The addition of electric and magnetic forces between the particles creates a rich interplay, allowing a wide range of strange and wonderful phenomena to occur. Some of these are well-known to most: lightning, electric sparks, fluorescent lamps, the Sun and the stars, and even the *aurora borealis* – the northern lights – are examples of plasmas. In fact, a majority of the visible matter in the universe is in the plasma state. The study of plasmas is a vast field of research, ranging from astrophysical research and space physics, through fusion-energy research to various industrial and medical applications.

Runaway is a phenomenon which occurs in any plasma in the presence of a sufficiently strong electric field. It is a process related to dielectric breakdown, which occurs when electric sparks are created. Runaway breakdown occurs in laboratory plasmas, such as those in tokamak fusion devices [1], as well as in lightning discharges during thunderstorms [2], and in astrophysical plasmas, such as solar flares [3]. In these scenarios, a subpopulation of particles – typically electrons, which are the lightest – are accelerated by the electric field to energies significantly higher than the thermal energy, at which point they will emit large amounts of radiation that will be visible to an observer.

The phenomenon of runaway can be understood by considering the frictional drag force due to collisions which acts on a charged particle moving through a plasma that is near thermodynamic equilibrium. Fric-

tion in plasmas is a non-monotonic function of speed: at low speed, the drag steadily grows in magnitude as the speed increases; however, above the thermal speed of the particles, the drag force will instead decrease in magnitude as the speed increases further. In the absence of an electric field, the friction force on the thermal particles will be balanced by velocity-space diffusion induced by collisions, which tends to increase the width of the velocity distribution. An equilibrium between friction and diffusion is reached when the distribution takes the Maxwellian form, $f_M = n(m/2\pi T)^{3/2} \exp(-mv^2/2T)$, where m, n and T are the mass, number density and temperature (in energy units, throughout this work) of the species, and v is the speed.

In the presence of an electric field which acts to accelerate charged particles, an electron with sufficiently high initial speed will experience an unbounded acceleration to highly relativistic energies, where the electrons move at close to the speed of light. At these energies, competing physical effects become important, such as radiation losses caused by the rapidly accelerated motion experienced by the particles when moving in electromagnetic fields (leading to synchrotron radiation) or in collisions (causing bremsstrahlung emission). Figure 1.1 illustrates the forces which act on a runaway electron.

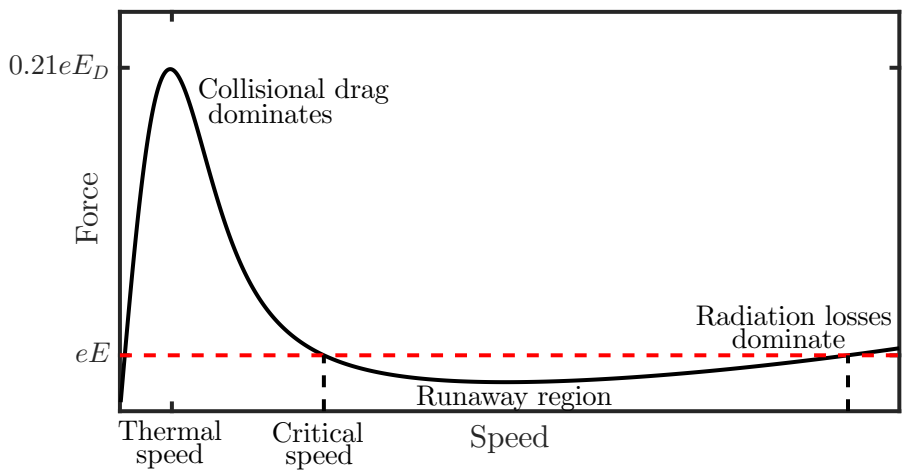

Figure 1.1: The speed-dependent force acting on a particle in a plasma, showing friction due to collisions and radiation (solid, black) and acceleration by an electric field (dashed, red). Not to scale (the speed where radiation losses become important can be thousands of times larger than the thermal speed).

1.1 Runaway generation

Historically, the basic runaway phenomenon was first encountered by Wilson in the early 20th century, who considered the acceleration of β-rays moving through a medium under the influence of a strong DC electric field [4, 5], having electron acceleration in thunderclouds in mind. He demonstrated that in a sufficiently strong constant electric field, energetic electrons would gain kinetic energy at an increasing rate as they accelerate. In 1926, in *The Internal Constitution of the Stars*, Eddington coined the term "runaway" electron to describe this "Wilson effect" [6].

Primary generation

Among the earliest[1] theoretical studies of runaway in plasmas was the work by Dreicer [8] in 1959. He considered the total friction force between two Maxwellian particle species moving uniformly with a given speed relative to each other. When accelerated by a sufficiently strong electric field, of order of the so-called Dreicer field

$$E_D = \frac{n_e e^3 \ln \Lambda}{4\pi\varepsilon_0^2 T_e},$$

the electric force overcomes the maximum frictional force, and he concluded that the particles would "run away" towards infinite energy (given infinite time). The Coulomb logarithm $\ln \Lambda$ is a plasma parameter which typically takes values 10-20 in the applications we consider [9].

In 1964, Kruskal and Bernstein [10] rigorously treated the runaway problem with an analytic solution to the kinetic equation (albeit using a simplified model for collisions). They solved the kinetic equation with an asymptotic technique, matching approximate solutions across five regions in momentum space, thereby obtaining expressions for the shape of the velocity distribution of runaway electrons and the rate at which new runaways are generated (here called the runaway growth rate). It was found that all electrons moving with a velocity above a critical velocity v_c – the velocity above which the electric field becomes stronger than friction – will run away towards infinite energy. In addition, diffusion would supply the runaway region ($v > v_c$) with new particles from the bulk at a constant rate. This mechanism of runaway generation is referred to as primary generation, or *Dreicer generation*.

[1] Earlier efforts have been briefly reviewed by Harrison [7].

Early work on runaways primarily considered the initial generation of runaways at relatively low, non-relativistic speeds. A full description of electron runaway requires the use of a relativistic kinetic equation, a scenario which was first analyzed by Connor and Hastie [11] in 1975. They extended the method of Kruskal and Bernstein to account also for relativistic effects. Unlike the case of non-relativistic runaway, where the frictional force appears to tend towards zero for large speeds, the friction in the relativistic model attains a minimum value, corresponding to a critical (Connor-Hastie) electric field

$$E_c = \frac{n_e e^3 \ln\Lambda}{4\pi\varepsilon_0^2 m_e c^2}.$$

This electric field is smaller than the Dreicer field by the factor $T/m_e c^2$. The result of the Connor-Hastie analysis is an explicit expression for the primary runaway growth rate $\gamma = (\partial n_{\mathrm{RE}}/\partial t)_{\mathrm{primary}}$, given by

$$\gamma = C\frac{n_e}{\tau_{ee}}\left(\frac{E}{E_D}\right)^{-\frac{3}{16}(1+Z_{\mathrm{eff}})h} \exp\left[-\lambda\frac{E_D}{4E} - \sqrt{\eta\frac{(1+Z_{\mathrm{eff}})E_D}{E}}\right], \quad (1.1)$$

$$\lambda = 8\frac{E^2}{E_c^2}\left[1 - \frac{1}{2}\frac{E_c}{E} - \sqrt{1-\frac{E_c}{E}}\right],$$

$$\eta = \frac{1}{4}\frac{E^2}{E_c(E-E_c)}\left[\frac{\pi}{2} - \arcsin\left(1-\frac{2E_c}{E}\right)\right]^2,$$

$$h = \frac{1}{3}\frac{1}{\frac{E}{E_c}-1}\left[\frac{E}{E_c} + 2\left(\frac{E}{E_c}-2\right)\sqrt{\frac{E}{E-E_c}} - \frac{Z_{\mathrm{eff}}-7}{Z_{\mathrm{eff}}+1}\right].$$

The prefactor C is an order-unity parameter which is undetermined by the asymptotic analysis, but tends to be nearly constant $C \sim 0.3$ [14]. The three parameters λ, η and h all approach unity when E/E_c becomes large, so that the non-relativistic limit $E \gg E_c$ is obtained by setting $\lambda = \eta = h = 1$, correctly reducing to the Kruskal-Bernstein result. The effective charge of the plasma is denoted $Z_{\mathrm{eff}} = \sum_i n_i Z_i^2/n_e$, and $\tau_{ee} = 4\pi\varepsilon_0^2 m_e^2 v_{\mathrm{Te}}^3/(n_e e^4 \ln\Lambda)$ is the electron thermal collision time, with the electron thermal speed $v_{Te} = \sqrt{2T_e/m_e}$. It is found that the runaway growth rate is exponentially sensitive to the electric field, the dominant scaling following approximately $\gamma \propto \exp(-E_D/4E)$. Unless the electric field is a significant fraction of the Dreicer field E_D – typically a few percent – the primary generation mechanism will accelerate only a negligible number of runaways.

Secondary generation

Another mechanism for runaway generation was originally proposed by Sokolov [12] in 1979, which is often referred to as *secondary*, *avalanche* or *knock-on* generation of runaways. For a given electric field $E > E_c$, there is a critical speed v_c above which electrons will almost certainly become runaway accelerated. Whereas in the primary generation mechanism, thermal electrons are fed into the runaway region $v > v_c$ by a nearly continuous collisional diffusion, the secondary generation mechanism supplies fast electrons through single large-angle collisions between existing runaways and the thermal population. Since the rate at which this occurs is directly proportional to the number of runaways present, one may expect that in a knock-on-dominated discharge the number of runaways will grow exponentially in time, hence being referred to as a runaway avalanche.

In a seminal paper by Rosenbluth and Putvinski [13] in 1997 (following notable developments by Jayakumar *et al.* [14]), the effect of large-angle collisions on the runaway rate was detailed. By solving the kinetic equation in various limits, whilst including a source term describing the momentum-space distribution of knock-on electrons, they obtained an avalanche growth rate $\Gamma = n_{\mathrm{RE}}^{-1} \left(\partial n_{\mathrm{RE}}/\partial t\right)_{\mathrm{secondary}}$ given by the asymptotically-matched formula

$$\Gamma = \frac{1}{\tau_c \ln\Lambda} \sqrt{\frac{\pi\rho}{3(Z_{\mathrm{eff}}+5)}} \frac{\frac{E}{E_c} - 1}{\sqrt{1 - \frac{E_c}{E} + \frac{4\pi(Z_{\mathrm{eff}}+1)^2}{3\rho(Z_{\mathrm{eff}}+5)(E^2/E_c^2 + 4/\rho^2 - 1)}}}, \tag{1.2}$$

$$\rho = \frac{3}{4}\int_0^1 \frac{\lambda \mathrm{d}\lambda}{\oint \sqrt{1-\lambda b(\theta)}\mathrm{d}\theta/2\pi} \approx \frac{1}{1 + 1.46\sqrt{\frac{r}{R}} + 1.72\frac{r}{R}}.$$

Here, $\tau_c = 4\pi\varepsilon_0^2 m_e^2 c^3/(n_e e^4 \ln\Lambda)$ is the relativistic electron collision time, and the neoclassical function ρ represents the effects of an inhomogeneous magnetic field, with the approximate equality corresponding to the large-aspect ratio limit $r \ll R$ in a tokamak. In the important limit $E/E_c \gg \sqrt{1+Z_{\mathrm{eff}}}$ and large aspect ratio, the avalanche growth rate takes the relatively simple form

$$\Gamma \approx \frac{1}{\tau_c \ln\Lambda \sqrt{Z_{\mathrm{eff}}+5}} \left(\frac{E}{E_c} - 1\right). \tag{1.3}$$

The total rate at which a runaway population grows, given by the

sum of primary and secondary generation, is

$$\frac{\mathrm{d}n_{\mathrm{RE}}}{\mathrm{d}t} = \gamma + n_{\mathrm{RE}}\Gamma.$$

In a constant electric field, the generation rate will initially be dominated by primary generation, so that $n_{\mathrm{RE}} \approx \gamma t$. Avalanche generation will become dominant once $\gamma = n_{\mathrm{RE}}\Gamma \approx \gamma t\Gamma$, i.e. after approximately one avalanche time $t_{\mathrm{ava}} = 1/\Gamma$. Note that the net force acting on a runaway electron is approximately $\mathrm{d}p/\mathrm{d}t = e(E - E_c)$, meaning that in one avalanche time a runaway has time to accelerate to a momentum

$$p = e(E - E_c)t_{\mathrm{ava}} \approx m_e c \ln\Lambda\sqrt{Z_{\mathrm{eff}} + 5},$$

which is independent of the electric-field strength [14]! Consequently, by the time that the fastest electron in the plasma has reached an energy of $\frac{1}{2}\ln\Lambda\sqrt{Z_{\mathrm{eff}} + 5}\,\mathrm{MeV}$, avalanche is the dominant runaway generation mechanism. As a corollary, in runaway discharges where significant avalanche multiplication occurs the runaway electron population is always ultrarelativistic with average energies in the 10 MeV range, unless there are energy loss mechanisms that can compete with the electric field without deconfining the runaways.

1.2 Runaway in tokamaks

Runaways are of particular interest in magnetic-fusion research, where they pose a great threat to the successful operation of tokamaks [15, 16]. The tokamak is a promising concept for fusion-energy reactors [17, 18], which confine a plasma by a magnetic field and heat it to several hundred million Kelvin. At these temperatures nuclear fusion reactions spontaneously occur, releasing large amounts of energy which is then available for generation of electricity. The magnetic field is partially generated by driving a strong current of several mega-ampere through the plasma, with the downside that this is then available for conversion into a runaway-carried current. The mechanism for this conversion is the runaway breakdown, which typically occurs during so-called disruptions [15, 19, 20] which are sudden events where heat confinement is lost. During these disruptions the plasma loses its energy and cools rapidly on a timescale of milliseconds [18] in a thermal quench, sometimes to less than one-thousandth of its original temperature. Due to its size, in a tokamak the total plasma current cannot change on the thermal-quench

time scale. The temperature reduction is associated with a massive decrease in the electrical conductivity of the plasma, thereby inducing strong electric fields in the vessel and plasma in order to maintain the current. These fields are often large enough to enable runaway breakdown to occur. The occurence of runaway in tokamaks was first pointed out in the literature by Gibson [21] in 1959, and has since been regularly observed and studied in a large number of tokamaks.

Avalanche runaway multiplication will often dominate the runaway generation, although initiation of the avalanche requires the presence of an initial seed population of runaways. This can be provided either by Dreicer generation, as described above, or by so-called hot-tail generation [22, 23, 24, 25, 26]. This third generation mechanism is enabled by the rapid temperature change that occurs during disruptions. If the cooling is sufficiently fast – comparable to the thermal collision time of the plasma – the fastest particles in the tail of the thermal distribution (which experience a weaker drag force) will maintain their initial energy. During the cooling their speeds may at some point exceed the critical speed for runaway generation, and thus they can become runaway accelerated.

It can be shown that, if there is an initial seed population $n_{\mathrm{RE},0}$ of runaways, avalanche multiplication will increase this number to approximately $n_{\mathrm{RE}} \sim \exp\left(2.5I[\mathrm{MA}]\right) n_{\mathrm{RE},0}$ before the electric field has decayed [15], where $I[\mathrm{MA}]$ is the original plasma current in MA. While the multiplication factor is fairly small in present-day experiments (of order 10^4 [15] in the JET tokamak [27, 28], the biggest experiment to date), in future tokamaks such as ITER [29] this implies a devastating number of 10^{16} or greater [15]. Because of this immense number, runaway-electron dynamics and disruption mitigation are fields of active study. Recent reviews can be found in Refs. [30, 31, 32, 33, 34]. The avalanche multiplication factor is exponentially sensitive to the avalanche growth rate Γ, and in order to accurately predict the final runaway current the large-angle collisions must be modelled precisely. In Paper A we therefore present a linearized Boltzmann operator which generalizes the knock-on models that have previously been used, allowing more accurate generation rates to be calculated than was previously possible.

At highly relativistic (multi-MeV) energies, additional effects such as radiation losses become important for the dynamics of the fast electrons. These effects only weakly impact runaway generation which typically occurs at non-relativistic speeds, but are particularly important during

the termination phase of a runaway beam where the current decays with time. Accurate models for radiation losses are then needed in order to understand the energy distribution of the runaway population, as well as the threshold electric field below which runaways slow down. This motivated the study presented in Paper B, where a model for bremsstrahlung losses treated as binary large-angle collisions is introduced.

The qualitative features of the basic runaway phenomenon in plasmas can thus be summarized as:

- Runaway is only possible for electric fields exceeding the critical field, $E > E_c$.
- Primary (Dreicer) runaway generation is exponentially sensitive to electric field, and only gives an appreciable growth rate when $E \gtrsim 0.03 E_D$.
- Secondary (avalanche) runaway generation depends weakly on electric field and is caused by knock-on collisions, requiring a population of runaways to already be present in the plasma. When avalanche generation is significant the average runaway energy is in the 10 MeV range, and vice versa.
- Hot-tail runaway generation occurs during a rapid temperature drop, and describes significant conversion of previously thermal electrons into runaways even when $E \lesssim 0.01 E_D$ at all times.
- Once the entire plasma current is carried by runaways, the system tends to be at marginal stability where the electric field must be near the avalanche threshold field (E_c in the ideal theory) wherever the current density is non-vanishing [35]. This sets the decay time of a runaway beam in a tokamak to roughly $\mathrm{d}I/\mathrm{d}t \sim (10\,\mathrm{kA/s}) \times \ln\Lambda\, n/(10^{20}\,\mathrm{m}^{-3})$ in the absence of radial particle transport, where n is the electron density.

Disruption mitigation

Due to the expected detrimental effect of a large unmitigated runaway beam in reactor-scale tokamaks, electron runaway is a question of critical importance for the ITER programme [15]. The demands of the disruption mitigation system are multifaceted [36]: during the thermal quench, where the plasma rapidly releases its thermal energy, the energy flux density to the wall must be kept below a certain threshold

by distributing the energy loads in space and time. During the current quench that follows, the poloidal magnetic energy of the plasma is released, either directly into the first wall via eddy currents that are induced or radiated from the plasma, or into the formation of a runaway electron beam. The current quench must be sufficiently rapid that significant halo currents causing large electromagnetic forces are avoided, but sufficiently slow that excessive runaway generation is also avoided; the energy transferred to runaway electrons is of particular concern, because it will eventually be deposited into the wall both locally and within a short time interval. As a result, runaways can cause immense localized damage to plasma-facing components, forcing extensive (and expensive) maintenance of the tokamak.

The current disruption mitigation plan for ITER revolves around massive material injection where large amounts of high-Z matter is injected into the plasma, which will reduce the current-quench time and contribute to radiating the energy content of the plasma. Large uncertainties still surround the formation of the runaway beam during disruptions [16], however, calling for an urgent need to develop more accurate models for runaway as well as disruption dynamics. This spurred the study presented in Paper E, where we describe a model for electron collisions with partially ionized impurities, which is essential in order to predict the generation and decay rate – and indeed the distribution function – of runaway electrons in tokamak disruption scenarios.

1.3 Ion runaway

Runaway acceleration of ions – instead of the nowadays more commonly studied electron runaway – was first invoked in order to explain experimental observations at the Zeta device [21] in 1959. In 1972, Furth and Rutherford [37] used an asympotic technique similar to that used for electron runaway in order to obtain an analytic solution of the ion drift-kinetic equation. Their treatment, however, provided only limited information about the runaway growth rate in most scenarios due to the more complicated structure of the ion kinetic equation. A limited time-dependent solution of the ion kinetic equation was more recently developed in order to explain observations at the Mega Ampere Spherical Tokamak [38, 39, 40, 41]. Simpler test-particle methods have also been used to study the ion runaway phenomenon in astrophysical contexts [42]. The lack of widely applicable analytic results has motivated

a numerical study of the ion drift-kinetic equation, which is presented in Paper D. Experimentally observed ion acceleration in the Madison Symmetric Torus reversed-field pinch has lead to recent work where similar methods have been employed [43, 44].

1.4 Outline

Chapter 2 contains an introduction to the kinetic theory of plasmas, which describes the phase-space dynamics of charged particles. The theory presented here covers the physics required to understand the basic runaway phenomenon, but is also the foundation upon which further extensions of the theory can be developed. In chapter 3, we discuss the radiation emitted by runaways. We develop the runaway kinetic theory by describing a model for the effect of bremsstrahlung emission based on the Boltzmann collision operator. We also present a synthetic diagnostic for the radiation that a runaway population will emit, focusing on synchrotron radiation and bremsstrahlung. The method predicts what a radiation detector would measure when observing a tokamak plasma containing runaway electrons. The theory for the runaway of positively charged particle species requires a modified treatment compared to electron runaway; the theory for runaway of ions and positrons is summarized in chapter 4. Finally the thesis is summarized in chapter 5, where we also present an outlook for future work in the field of runaway.

Chapter 2

The kinetic equation

A detailed study of runaway particles requires the resolution of their momentum-space structure, accounting for the randomizing collisions in an accurate way. This is achieved using a kinetic equation, which provides a full description of the time evolution of the distribution function $f_a(t, \mathbf{x}, \mathbf{p})$ of a particle species a, where t is time, $\mathbf{x}$ is the particle position, $\mathbf{p} = m_a \mathbf{v}/\sqrt{1 - v^2/c^2}$ is the momentum and $\mathbf{v}$ is the velocity, with $v = |\mathbf{v}|$. The distribution function is the particle density function in phase space, defined such that $n_a(t, \mathbf{x}) = \int \mathrm{d}\mathbf{p}\, f_a(t, \mathbf{x}, \mathbf{p})$ is the number density, and $N_a(t) = \int \mathrm{d}\mathbf{x}\, n_a(t, \mathbf{x})$ is the total number of particles of species a. In the absence of collisions, the distribution function describes particles moving along trajectories $\mathbf{x} = \mathbf{x}(t)$ and $\mathbf{p} = \mathbf{p}(t)$, governed by the equations of motion for a charged particle

$$\begin{aligned} \frac{\mathrm{d}\mathbf{x}}{\mathrm{d}t} &= \mathbf{v}, \\ \frac{\mathrm{d}\mathbf{p}}{\mathrm{d}t} &= q_a\big(\mathbf{E} + \mathbf{v} \times \mathbf{B}\big), \end{aligned}$$

where q_a is the electrical charge of species a, $\mathbf{E}$ the electric field and $\mathbf{B}$ the magnetic field. The continuity equation in phase space is [45]

$$0 = \frac{\mathrm{d}f_a}{\mathrm{d}t} = \frac{\partial f_a}{\partial t} + \mathbf{v} \cdot \frac{\partial f_a}{\partial \mathbf{x}} + q_a\big(\mathbf{E} + \mathbf{v} \times \mathbf{B}\big) \cdot \frac{\partial f_a}{\partial \mathbf{p}}, \tag{2.1}$$

where the electric and magnetic fields are given by the charge and current distribution of the plasma according to Maxwell's equations,

$$\begin{aligned} \mathbf{E}(t, \mathbf{x}) &= -\nabla\phi - \frac{\partial \mathbf{A}}{\partial t}, \\ \mathbf{B}(t, \mathbf{x}) &= \nabla \times \mathbf{A}. \end{aligned}$$

When the time variations of the plasma are slow compared to the transit time of light across its extent, the electromagnetic potential functions are given by

$$\phi(t,\mathbf{x}) = \frac{1}{4\pi\varepsilon_0}\int \mathrm{d}\mathbf{x}'\,\frac{\rho(t,\mathbf{x}')}{|\mathbf{x}-\mathbf{x}'|},$$
$$\mathbf{A}(t,\mathbf{x}) = \frac{\mu_0}{4\pi}\int \mathrm{d}\mathbf{x}'\,\frac{\mathbf{j}(t,\mathbf{x}')}{|\mathbf{x}-\mathbf{x}'|},$$

where the charge ρ and current $\mathbf{j}$ within the plasma are in turn determined by the distribution functions,

$$\rho(t,\mathbf{x}) = \sum_b q_b \int \mathrm{d}\mathbf{p}\, f_b(t,\mathbf{x},\mathbf{p}),$$
$$\mathbf{j}(t,\mathbf{x}) = \sum_b q_b \int \mathrm{d}\mathbf{p}\,\mathbf{v} f_b(t,\mathbf{x},\mathbf{p}),$$

with the sum taken over all particle species b present in the plasma. In order to obtain a useful kinetic equation, Eq. (2.1) needs to be ensemble-averaged over macroscopically equivalent systems. The distribution function will then become a smooth function, but the microscopic interactions between the discrete particles in the plasma will need to be accounted for by the addition of a new term [46], which is called the *collision operator* C, or the collision integral (as it generally takes the form of an integral operator). The kinetic equation then takes the form

$$\frac{\partial f_a}{\partial t} + \mathbf{v}\cdot\frac{\partial f_a}{\partial \mathbf{x}} + q_a\big(\mathbf{E}+\mathbf{v}\times\mathbf{B}\big)\cdot\frac{\partial f_a}{\partial \mathbf{p}} = \sum_b C_{ab}\{f_a, f_b\}, \tag{2.2}$$

where $\mathbf{E}$ and $\mathbf{B}$ now denote the macroscopic fields, not including fluctuations caused by individual particles which are instead captured by the collision operator C. Throughout this thesis, we mainly focus on the simplest scenario that exhibits the runaway phenomenon: an infinite homogeneous plasma with an electric field in a constant direction (although allowed to vary in amplitude with time). In this case we can suppress the space variables and write $f_a = f_a(t,\mathbf{p})$, and introduce a spherical momentum coordinate system (p,θ,φ) aligned with the electric field, in which the azimuthal angle φ is referred to as the gyroangle and the longitudinal angle θ is referred to as the pitch-angle. The kinetic equation then becomes

$$\frac{\partial f_a}{\partial t} + q_a E\left(\xi\frac{\partial f_a}{\partial p} + \frac{1-\xi^2}{p}\frac{\partial f_a}{\partial \xi}\right) = \sum_b C_{ab}\{f_a, f_b\}, \tag{2.3}$$

where $\xi = \cos\theta = \mathbf{p}\cdot\mathbf{E}/pE$. This equation allows us to study the effects of various contributions in the collision operator C on the dynamics of the runaway particles. The model also approximately describes the local dynamics of runaways near the magnetic axis in a tokamak, if E is taken to be the component of the electric field parallel to the magnetic field and the pitch ξ is defined relative to the magnetic field.

An essential part of the description of runaway electrons is the collision operator. This term in the kinetic equation describes the effect of microscopic particle-particle interactions, in contrast to the macroscopic interactions with the electromagnetic field set up by the charge distribution in the plasma or by external sources. The collisions drive the particle distributions towards thermal equilibrium by always increasing entropy in the system, and this is the restoring effect which needs to be overcome by the electric field in order to generate runaway particles. Therefore the details of the collision operator can be expected to strongly influence the description of the runaway process.

In this chapter we will provide a detailed discussion of the collision operator, revealing a unified picture of small-angle collisions, knock-on collisions and bremsstrahlung radiation in the same framework. We shall begin by presenting in more detail how the collision operator can be obtained.

2.1 BBGKY hierarchy and the kinetic equation

A systematic framework for obtaining kinetic equations was initially developed by Bogolyubov, Born, Green, Kirkwood and Yvon (BBGKY) [47, 48, 49, 50, 51]. The starting point of their analysis is the Liouville theorem [52], which deterministically describes the time evolution of an N-body system according to Hamiltonian mechanics. The system is fully described by the phase space density function $f_N(t, \mathbf{x}_1, \mathbf{p}_1, ..., \mathbf{x}_N, \mathbf{p}_N)$ giving the location and momentum of all its constituents. A kinetic equation describes the time evolution of the distribution function, which is defined as $f(t, \mathbf{x}, \mathbf{p}) = \int \mathrm{d}\mathbf{x}_2\mathrm{d}\mathbf{p}_2 \cdots \mathrm{d}\mathbf{x}_N\mathrm{d}\mathbf{p}_N\, f_N(t, \mathbf{x}, \mathbf{p}, \mathbf{x}_2, \mathbf{p}_2, ..., \mathbf{x}_N, \mathbf{p}_N)$. Note that, while this definition appears to single out the particle with subscript 1 as special, the particles described by the phase-space density function are identical, and hence it is symmetric in all indices. That is, non-identical particle species are each described by their own distribution function.

The Liouville equation [53] for a species interacting pair-wise with a

central potential $V_{ij} = V(|\mathbf{x}_i - \mathbf{x}_j|)$, with the force on particle i being $\mathbf{F}_i = -\sum_{(j\neq i)=1}^{N} \partial V_{ij}/\partial \mathbf{x}_i$ (for simplicity assuming a single species and no magnetic interaction, which would require a generalized form of the potential), is given by

$$\frac{\partial f_N}{\partial t} + \sum_{i=1}^{N} \frac{\mathbf{p}_i}{m_a} \cdot \frac{\partial f_N}{\partial \mathbf{x}_i} - \sum_{i=1}^{N} \sum_{(j\neq i)=1}^{N} \frac{\partial V_{ij}}{\partial \mathbf{x}_i} \cdot \frac{\partial f_N}{\partial \mathbf{p}_i} = 0.$$

By integrating over all but s particle coordinates, a *reduced* phase space density, or the *s-particle correlation function*, can be defined as $f_s = \int \mathrm{d}\mathbf{x}_{s+1}\mathrm{d}\mathbf{p}_{s+1} \cdots \mathrm{d}\mathbf{x}_N \mathrm{d}\mathbf{p}_N \, f_N$. Here, $s = 1$ gives the distribution function in which we are most interested, and $s = N$ returns the full N-particle phase space density. When performing such an integration over the Liouville equation, an equation for the time-evolution of the reduced distribution function is obtained; however, the equation for $\partial f_s/\partial t$ invariably contains f_{s+1} due to the pair-wise interaction term. Thus, the time-evolution of the distribution function depends on the two-particle correlation function f_2, which in turn is affected by f_3, and so on. This set of coupled partial differential equations is called the BBGKY hierarchy. A systematic approximation scheme to close this set of equations was developed by Frieman [54], Sandri [55] and collaborators, which takes the form of a perturbation expansion in two parameters μ and η. These appear naturally when normalizing the equation to characteristic values of particle separation r_0, velocities v_0 and interaction strength V_0, and are given by

$$\mu = \frac{1}{n r_0^3},$$
$$\eta = \frac{V_0}{m v_0^2} \sim \frac{e^2}{4\pi\varepsilon_0 T r_0}.$$

Here $1/\mu$ is the number of particles in the interaction region (defined by a characteristic range r_0), and η is a measure of the strength of the interaction (described by the potential function V_0) compared to the kinetic energy. There are three domains of primary interest [56, 57] which can be described as (1) “dilute, short-range”, (2) “weak coupling” (small momentum transfer) and (3) “long-range”. These, respectively,

correspond to the choices (with ϵ a small expansion parameter)

$$\begin{aligned} &(1) \quad \mu = \mathcal{O}(\epsilon^{-1}), && \eta = \mathcal{O}(1), \\ &(2) \quad \mu = \mathcal{O}(1), && \eta = \mathcal{O}(\epsilon), \\ &(3) \quad \mu = \mathcal{O}(\epsilon), && \eta = \mathcal{O}(\epsilon). \end{aligned}$$

These lead, in turn, to (1) the so-called Boltzmann equation, (2) the Fokker-Planck equation and (3) the Balescu-Lenard (or Bogolyubov-Lenard-Balescu) equation. Plasmas are particularly pathological, as no specific ordering applies to the entire phase space. The long-range Coulomb interaction allows for collisions where any of the orderings may apply, depending on the impact parameter.

An analysis shows that the Balescu-Lenard operator takes a similar form to the Fokker-Planck operator, but where the dielectric constant of the plasma appears in the collision integral. This factor accounts for *dynamical screening* in the plasma, which ensures that collisions with impact parameter of order the Debye length $\lambda_\mathrm{D} = \sqrt{\varepsilon_0 T/ne^2}$ or greater are exponentially damped. This effect demonstrates the well-known behavior of Debye screening [17], where the electric field from a point charge in a plasma will be exponentially damped on a length scale λ_D by the rearrangement of the surrounding plasma. The Fokker-Planck collision operator diverges in the contribution from large-impact-parameter collisions, but by following Landau's prescription from the original derivation [58] to cut the integration off at impact parameters λ_D (which can be motivated by the Balescu-Lenard equation), one obtains a convergent integral. The contribution from small-angle collisions in the Fokker-Planck operator is then found to be larger than the contribution from large-angle collisions in the Boltzmann operator by a factor $\ln n\lambda_\mathrm{D}^3 \simeq \ln \Lambda$, the so-called Coulomb logarithm.

In this chapter we will not pursue a detailed analysis of the BBGKY hierarchy of equations. Instead, we will derive the Boltzmann and Fokker-Planck collision operators with heuristic arguments, based on an analysis of binary collisions. This method gives the same result as the more rigorous derivation from first principles, and also provides some physical insight into how we may view collisions in a plasma.

2.2 The Boltzmann collision operator

The Boltzmann equation was originally derived by Ludwig Boltzmann in the late nineteenth century [59, 60] in order to study the dynamics of

gases. As we indicated in the previous section, the Boltzmann equation for a plasma is valid when describing those large-angle collisions where the impact parameter is much smaller than the mean distance between particles in the plasma, that is for $\mu \gg 1$. The Boltzmann collision operator describes the rate-of-change of the distribution function due to binary collisions, and we shall briefly derive it here in a form that will be suited to our applications.

We describe a binary interaction with a differential cross-section $\mathrm{d}\sigma_{ab}(\mathbf{p}_1, \mathbf{p}_2; \mathbf{p}, \mathbf{p}')$ for particles a and b to be taken from initial momenta $\mathbf{p}$ and $\mathbf{p}'$, respectively, to final momenta $\mathbf{p}_1$ and $\mathbf{p}_2$, respectively. The cross-section is defined such that the total differential change of the phase-space particle density $\mathrm{d}n_a(t, \mathbf{x}, \mathbf{p}) = f_a(t, \mathbf{x}, \mathbf{p})\mathrm{d}\mathbf{p}$ due to these interactions in a time interval $\mathrm{d}t$ is

$$\begin{aligned}\left[\mathrm{d}n_a(\mathbf{p})\right]_{c,ab} = {} & f_a(\mathbf{p}_1) f_b(\mathbf{p}_2) g_\emptyset(\mathbf{p}_1, \mathbf{p}_2) \mathrm{d}\sigma(\mathbf{p}, \mathbf{p}'; \mathbf{p}_1, \mathbf{p}_2) \mathrm{d}\mathbf{p}_1 \mathrm{d}\mathbf{p}_2 \mathrm{d}t \\ & - f_a(\mathbf{p}) f_b(\mathbf{p}') g_\emptyset(\mathbf{p}, \mathbf{p}') \mathrm{d}\sigma(\mathbf{p}_1, \mathbf{p}_2; \mathbf{p}, \mathbf{p}') \mathrm{d}\mathbf{p} \mathrm{d}\mathbf{p}' \mathrm{d}t, \end{aligned} \tag{2.4}$$

where $\mathbf{p}_1$ and $\mathbf{p}_2$ are related to $\mathbf{p}$ and $\mathbf{p}'$ by the conservation of energy and momentum. The relativistic generalization of the relative speed $v_{\mathrm{rel}} = |\mathbf{v} - \mathbf{v}'|$, is the Møller relative speed $g_\emptyset(\mathbf{p}, \mathbf{p}') = \sqrt{(\mathbf{v} - \mathbf{v}')^2 - (\mathbf{v} \times \mathbf{v}')^2/c^2}$ [61]. The collision operator can formally be defined as

$$\begin{aligned} C_{ab}\{f_a, f_b\} \equiv {} & \left(\frac{\partial^2 n_a}{\partial t \partial \mathbf{p}}\right)_{c,ab} \\ = {} & \int \mathrm{d}\mathbf{p}_1 \, f_a(\mathbf{p}_1) \int \mathrm{d}\mathbf{p}_2 \, f_b(\mathbf{p}_2) g_\emptyset(\mathbf{p}_1, \mathbf{p}_2) \frac{\partial \sigma(\mathbf{p}, \mathbf{p}'; \mathbf{p}_1, \mathbf{p}_2)}{\partial \mathbf{p}} \\ & - f_a(\mathbf{p}) \int \mathrm{d}\mathbf{p}' \, f_b(\mathbf{p}') g_\emptyset(\mathbf{p}, \mathbf{p}') \sigma(\mathbf{p}, \mathbf{p}'), \end{aligned} \tag{2.5}$$

where the total cross-section $\sigma(\mathbf{p}, \mathbf{p}')$ is defined as

$$\sigma(\mathbf{p}, \mathbf{p}') = \int \mathrm{d}\mathbf{p}_1 \, \frac{\partial \sigma(\mathbf{p}_1, \mathbf{p}_2; \mathbf{p}, \mathbf{p}')}{\partial \mathbf{p}_1}.$$

A symmetric form is obtained in the special case of elastic collisions by utilizing the *principle of detailed balance* [61], which is a symmetry relation for the cross-section stating that

$$g_\emptyset(\mathbf{p}_1, \mathbf{p}_2) \mathrm{d}\sigma(\mathbf{p}, \mathbf{p}'; \mathbf{p}_1, \mathbf{p}_2) \mathrm{d}\mathbf{p}_1 \mathrm{d}\mathbf{p}_2 = g_\emptyset(\mathbf{p}, \mathbf{p}') \mathrm{d}\sigma(\mathbf{p}_1, \mathbf{p}_2; \mathbf{p}, \mathbf{p}') \mathrm{d}\mathbf{p} \mathrm{d}\mathbf{p}'.$$

Using this relation, which is valid for classical particles interacting with a central potential and also in the first order spin-averaged Born approximation in quantum mechanics [62, 63], Eq. (2.4) leads to

$$C_{ab}\{f_a, f_b\} = \int \mathrm{d}\mathbf{p}'\mathrm{d}\sigma(\mathbf{p}_1, \mathbf{p}_2;\, \mathbf{p}, \mathbf{p}')\, g_\emptyset(\mathbf{p}, \mathbf{p}')\times \\ \times \Big(f_a(\mathbf{p}_1) f_b(\mathbf{p}_2) - f_a(\mathbf{p}) f_b(\mathbf{p}')\Big). \quad (2.6)$$

This is the operator which is typically referred to as the Boltzmann operator, although we shall apply the term more generally here to any integral operator of the form of Eq. (2.5). In Eqs. (2.4), (2.5) and (2.6) the first – the gain term – describes the rate at which particles a of initial momentum $\mathbf{p}_1$ are scattered into $\mathbf{p}$, while the second – the loss term – describes the rate at which particles scatter away from $\mathbf{p}$.

Large-angle collision operator for runaways

The description of large-angle collisions is essential in order to understand runaway dynamics. The reason is that when the electric field is far below the Dreicer field $E_D = n_e \ln\Lambda e^3/(4\pi\varepsilon_0^2 T_e)$, no thermal electrons will spontaneously be runaway accelerated through the primary (Dreicer) mechanism. Large-angle collisions between highly energetic runaways and the bulk population can, however, even under such circumstances generate a significant number of new runaways. The electron-electron Boltzmann operator for collisions between runaways and thermal electrons must therefore be included in the kinetic equation in order to capture the runaway avalanche.

Two main approximations allow a significantly simpler collision operator to be obtained:

(i) The runaways are assumed to be few in number, so that the operator can be linearized around the thermal background. This is often the case; due to their high speed, runaways would carry a massive current whenever their number density is comparable to that of the bulk plasma (giga-ampere scale in tokamaks).

(ii) The thermal electrons are treated as stationary, which can be motivated by the fact that the operator is mainly important when $E \ll E_D$, at which point runaway speeds will far exceed the thermal speed.

In that case, the linearized electron-electron collision operator takes the form

$$C_{ee} = n_\mathrm{e} \int \mathrm{d}\boldsymbol{p}_1\, v_1 \frac{\partial \sigma_\mathrm{ee}}{\partial \boldsymbol{p}} f_\mathrm{e}(\boldsymbol{p}_1) \;-\; n_\mathrm{e} v \sigma_\mathrm{ee}(\boldsymbol{p}) f_\mathrm{e}(\boldsymbol{p}) \\ -\; n_\mathrm{e} \delta(\boldsymbol{p}) \int \mathrm{d}\boldsymbol{p}_1 v_1 \sigma_\mathrm{ee}(\boldsymbol{p}_1) f_\mathrm{e}(\boldsymbol{p}). \tag{2.7}$$

The differential cross-section for relativistic electron-electron collisions is given by the Møller cross-section, which in the laboratory frame takes the form [62]

$$\frac{\partial \sigma_{ee}}{\partial \mathbf{p}}(\mathbf{p}, \mathbf{p}';\, \mathbf{p}_1, \mathbf{p}_2) = \frac{\delta(\cos\theta_s - \xi^*(\gamma, \gamma_1))}{2\pi p \gamma} \frac{\partial \sigma_{ee}}{\partial \gamma}(\gamma, \gamma_1), \tag{2.8}$$

$$\frac{\partial \sigma_{ee}}{\partial \gamma}(\gamma, \gamma_1) = \frac{2\pi r_0^2 \gamma_1^2}{(\gamma_1^2 - 1)(\gamma - 1)^2 (\gamma_1 - \gamma)^2} \Bigg((\gamma_1 - 1)^2 \\ - \frac{(\gamma - 1)(\gamma_1 - \gamma)}{\gamma_1^2} \Big[2\gamma_1^2 + 2\gamma_1 - 1 - (\gamma - 1)(\gamma_1 - \gamma) \Big] \Bigg). \tag{2.9}$$

Here, we have introduced the angles

$$\xi^*(\gamma, \gamma_1) = \sqrt{\frac{\gamma_1 + 1}{\gamma_1 - 1} \frac{\gamma - 1}{\gamma + 1}}, \\ \cos\theta_s = \frac{\mathbf{p}_1 \cdot \mathbf{p}}{p_1 p}, \tag{2.10}$$

and the delta function of the differential cross-section, relating the scattering angle θ_s to the energy transfer, arises due to the conservation of momentum and energy in elastic collisions. The classical electron radius is denoted $r_0 = e^2/(4\pi\varepsilon_0 m_e c^2) \approx 2.8 \cdot 10^{-15}\,\mathrm{m}$. The collision operator can then be further simplified under the additional assumption that

(iii) The runaway population is cylindrically symmetric in momentum space, fulfilling the conditions under which Eq. (2.3) was derived.

Expanding the electron distribution function in Legendre polynomials,

$$f_e(\mathbf{p}) = \sum_L f_L(p) P_L(\cos\theta), \tag{2.11}$$

then allows the linearized large-angle collision operator to be written

$$C_{ee}(\mathbf{p}) = \sum_L C_L(p) P_L(\cos\theta), \tag{2.12}$$

$$\begin{aligned} C_L(p) = {} & \frac{(m_\mathrm{e}c)^{-3}}{2\tau_\mathrm{c}\ln\Lambda}\frac{1}{\gamma p}\int_{q_0}^{\infty}\mathrm{d}p_1\,\frac{p_1^3}{\gamma_1}f_L(p_1)P_L(\xi^*)\Sigma(\gamma,\gamma_1) \\ & - \frac{1}{4\tau_\mathrm{c}\ln\Lambda}\frac{v}{c}f_L(p)\int_{\gamma_\mathrm{m}}^{\gamma+1-\gamma_\mathrm{m}}\mathrm{d}\gamma_1\,\Sigma(\gamma_1,\gamma) \\ & - \frac{(m_\mathrm{e}c)^{-1}}{4\tau_\mathrm{c}\ln\Lambda}\delta_{L,0}\frac{\delta(p)}{p^2}\int_{q_0}^{\infty}\mathrm{d}p'\,\frac{p'^3}{\gamma'}f_0(p')\int_{\gamma_\mathrm{m}}^{\gamma'+1-\gamma_\mathrm{m}}\mathrm{d}\gamma_1\,\Sigma(\gamma_1,\gamma'), \\ q_0 = {} & m_e c\sqrt{(\gamma+\gamma_m-1)^2-1}, \\ \frac{1}{\tau_c} = {} & \ln\Lambda\frac{n_e}{4\pi}\frac{e^4}{\varepsilon_0^2 m_e^2 c^3}. \end{aligned}$$

Here, we have truncated the collision operator so that it only accounts for those collisions where the secondary electron receives a kinetic energy greater than $m_e c^2(\gamma_m - 1)$, corresponding to a cut-off momentum $p_m = m_e c\sqrt{\gamma_m^2 - 1}$. This operator, which is derived in Paper A, still identically conserves electron density, momentum and energy. In Paper A we study its predictions for runaway avalanche generation and compare it to previous studies which have imposed further assumptions on the distribution function. One such example is the widely used model studied by Rosenbluth and Putvinski [13], where the runaway electron distribution is taken as a delta function at infinite momentum and zero pitch angle in the evaluation of the Boltzmann operator. In that case, the linearized electron-electron Boltzmann collision operator reduces to the remarkably simple form

$$C_\mathrm{RP}(\mathbf{p}) = n_\mathrm{RE}\frac{\delta[\cos\theta - \xi^*(\gamma,\infty)]}{4\pi\tau_c\ln\Lambda}\frac{(m_e c)^3}{p^2}\frac{\partial}{\partial p}\frac{1}{1-\gamma}, \tag{2.13}$$

$$n_\mathrm{RE} = \int_{p>p_c} f_e\,\mathrm{d}\mathbf{p}. \tag{2.14}$$

This operator refers explicitly to the runaway density and to the critical momentum which defines a runaway; in practice, the details of the definition are often unimportant as long as p_c is chosen to be significantly larger than the thermal momentum but negligible compared to the average runaway momentum.

2.3 The Fokker-Planck collision operator

When the interaction distance is significant compared to the mean particle separation, but the interaction is weak, the appropriate collision term is the Fokker-Planck operator, rather than the Boltzmann operator. However, as we will now show, the Fokker-Planck operator can in fact be derived from the Boltzmann operator in the limit of small momentum transfers in the collisions. That the seemingly opposite description of weak interactions in the Fokker-Planck picture can be contained in the Boltzmann picture of binary collisions appears counter-intuitive. It can, however, be physically understood by the fact that the small momentum transfers described by the Fokker-Planck operator only negligibly change the particle momentum in a single collision; then the net effect of the many-body interaction can be viewed as a linear superposition of pairwise momentum transfers [64].

The procedure is as follows: a general integral moment of the Boltzmann operator of a test function ϕ is given by

$$J[\phi] = \int \mathrm{d}\mathbf{p}\, \phi(\mathbf{p}) C_{ab} = \int \mathrm{d}\mathbf{p} \int \mathrm{d}\mathbf{p}' \mathrm{d}\sigma(\mathbf{p}_1, \mathbf{p}_2; \mathbf{p}, \mathbf{p}')\, f_a(\mathbf{p}) f_b(\mathbf{p}') \times g_{\text{ø}}(\mathbf{p}, \mathbf{p}') \Big[\phi(\mathbf{p}_1) - \phi(\mathbf{p})\Big],$$

which is most easily seen by integrating Eq. (2.4) and switching names of the dummy variables $\mathbf{p}_1$ and $\mathbf{p}_2$ in the first term with $\mathbf{p}$ and $\mathbf{p}'$, respectively. For convenience we will suppress the arguments of $\mathrm{d}\sigma$ and $g_{\text{ø}}$ as they will remain unchanged for the rest of the calculation. Here we introduce the small-momentum-transfer argument: the integral is assumed to be dominated by the contribution from $\mathbf{p}_1 \approx \mathbf{p}$. We then Taylor expand

$$\phi(\mathbf{p}_1) - \phi(\mathbf{p}) \simeq (\mathbf{p}_1 - \mathbf{p}) \cdot \frac{\partial \phi(\mathbf{p})}{\partial \mathbf{p}} + \frac{(\mathbf{p}_1 - \mathbf{p})(\mathbf{p}_1 - \mathbf{p})}{2} : \frac{\partial \phi(\mathbf{p})}{\partial \mathbf{p} \partial \mathbf{p}},$$

where we use dyadic notation such that the rank-2 tensor $\mathsf{T} = \mathbf{ab}$ has components $T_{ij} = a_i b_j$. By introducing the quantities

$$\Delta\mathbf{p} = \mathbf{p}_1 - \mathbf{p},$$

$$\mathbf{A} = \int \mathrm{d}\mathbf{p}'\, g_{\text{ø}} f_b(t, \mathbf{p}') \int \mathrm{d}\sigma\, \Delta\mathbf{p}, \tag{2.15}$$

$$\mathsf{D} = \int \mathrm{d}\mathbf{p}'\, g_{\text{ø}} f_b(t, \mathbf{p}') \int \mathrm{d}\sigma\, \Delta\mathbf{p}\Delta\mathbf{p}, \tag{2.16}$$

integrating by parts twice yields

$$J[\phi] = \int \mathrm{d}\mathbf{p}\, \phi(\mathbf{p}) \left[\frac{\partial}{\partial \mathbf{p}} \cdot \left(-\mathbf{A}(t,\mathbf{p}) f_a(t,\mathbf{p}) + \frac{1}{2} \frac{\partial}{\partial \mathbf{p}} \cdot \left[\mathsf{D}(t,\mathbf{p}) f_a(t,\mathbf{p}) \right] \right) \right].$$

As this equality holds for any ϕ, the small-momentum-transfer assumption therefore leads to the well-known Fokker-Planck operator [65, 66]

$$C_{ab}\{f_a, f_b\} = \frac{\partial}{\partial \mathbf{p}} \cdot \left[-\mathbf{A}_{ab}(t,\mathbf{p}) f_a(t,\mathbf{p}) + \frac{1}{2} \frac{\partial}{\partial \mathbf{p}} \cdot \left(\mathsf{D}_{ab}(t,\mathbf{p}) f_a(t,\mathbf{p}) \right) \right]. \tag{2.17}$$

For relativistic elastic electron-electron collisions, the Fokker-Planck operator was first given by Beliaev and Budker [67], with a direct derivation from Eqs. (2.15), (2.16) and (2.17) later given by Akama [68]. This Fokker-Planck operator can conveniently be expressed in the form

$$C_{ee}\{f_e, f_e\} = \frac{\partial}{\partial \mathbf{p}} \cdot \int \mathrm{d}\mathbf{p}'\, \mathcal{E} \cdot \left(\frac{\partial f_e(\mathbf{p})}{\partial \mathbf{p}} f_e(\mathbf{p}') - \frac{\partial f_e(\mathbf{p}')}{\partial \mathbf{p}'} f_e(\mathbf{p}) \right), \tag{2.18}$$

where the collision kernel $\mathcal{E}$ is the symmetric rank-2 tensor [69]

$$\mathcal{E} = 2\pi \left(\frac{e^2}{4\pi\varepsilon_0} \right)^2 \ln\Lambda \frac{\gamma'\gamma(1 - \mathbf{v}'\cdot\mathbf{v}/c^2)^2}{c\{[\gamma'\gamma - \mathbf{p}'\cdot\mathbf{p}/(m_e c)^2]^2 - 1\}^{3/2}} \times \Bigg\{ \left[\left(\gamma'\gamma - \frac{\mathbf{p}'\cdot\mathbf{p}}{m_e^2 c^2} \right)^2 - 1 \right] \mathsf{I} - \frac{\mathbf{p}\mathbf{p} + \mathbf{p}'\mathbf{p}'}{m_e^2 c^2} + \left(\gamma'\gamma - \frac{\mathbf{p}'\cdot\mathbf{p}}{m_e^2 c^2} \right) \frac{\mathbf{p}'\mathbf{p} + \mathbf{p}\mathbf{p}'}{m_e^2 c^2} \Bigg\},$$

where I is the unit tensor and $\gamma = \sqrt{1 + (p/m_e c)^2}$ is the relativistic Lorentz factor. In this expression, only the leading-order term in $\ln\Lambda$ has been retained, which corresponds to the small-angle contribution to the integrals (2.15) and (2.16).

General Fokker-Planck equation for stationary targets

The general Fokker-Planck operator given by (2.17) can be given in a more explicit form when considering collisions with stationary targets – which is often an appropriate approximation for runaways – and for isotropic collision processes which only depend on the energy transfer and deflection angle. In that case, it can be expressed as [70]

$$C_{ei} = \frac{\nu_D^{ei}(p)}{2} \frac{\partial}{\partial \xi} \left[\left(1 - \xi^2\right) \frac{\partial f_e}{\partial \xi} \right] + \frac{1}{p^2} \frac{\partial}{\partial p} \left[p^3 \left(\nu_s^{ei} f_e + \frac{\nu_\parallel^{ei} p}{2} \frac{\partial f_e}{\partial p} \right) \right], \tag{2.19}$$

where ν_D can be identified as the rate of deflection in pitch angle, ν_s the slowing-down frequency (so that the dynamical friction is given by $-\mathbf{p}\nu_s$) and $\nu_\parallel$ the rate of energy diffusion. For an arbitrary binary interaction, they are explicitly given by

$$\begin{aligned}
\nu_s &= \left\langle -\frac{\mathbf{p}\cdot\Delta\mathbf{p}}{p^2}\right\rangle - \nu_D + \nu_\parallel + \frac{1}{2}\frac{\partial(p\nu_\parallel)}{\partial p},\\
\nu_\parallel &= \frac{1}{p^4}\langle(\mathbf{p}\cdot\Delta\mathbf{p})^2\rangle,\\
\nu_D &= \frac{1}{2p^2}\langle|\Delta\mathbf{p}|^2 - \frac{1}{p^2}(\mathbf{p}\cdot\Delta\mathbf{p})^2\rangle.
\end{aligned} \tag{2.20}$$

The bracket $\langle A\rangle$ denotes the average rate of change of a quantity $A = A(\mathbf{p},\mathbf{p}_1)$ in a collision, and is for stationary targets defined by

$$\langle A\rangle(\mathbf{p}) = nv\int \mathrm{d}\mathbf{p}_1\,\frac{\partial\sigma_{ei}}{\partial\mathbf{p}_1}A(\mathbf{p},\mathbf{p}_1), \tag{2.21}$$

In terms of the scattering angle $\cos\theta_s = \mathbf{p}_1\cdot\mathbf{p}/p_1p$ we obtain the explicit expressions

$$\begin{aligned}
\nu_s &= \frac{1}{p^2}\langle p^2 - p_1p\cos\theta_s - \frac{1}{2}p_1^2\sin^2\theta_s\rangle + \frac{1}{2p^2}\frac{\partial}{\partial p}\left[p\langle(p-p_1\cos\theta_s)^2\rangle\right],\\
\nu_D &= \frac{1}{2p^2}\langle p_1^2\sin^2\theta_s\rangle,\\
\nu_\parallel &= \frac{1}{2p^2}\langle(p-p_1\cos\theta_s)^2\rangle.
\end{aligned} \tag{2.22}$$

If we then write $p_1 = p(1-\epsilon)$ and expand to second order in θ_s, we find

$$\begin{aligned}
\nu_s &= \langle\epsilon - \frac{1}{4}\epsilon^2\theta_s^2\rangle + \frac{1}{2p^2}\frac{\partial}{\partial p}\left[p^3\langle\epsilon^2 + \theta_s^2\epsilon(1-\epsilon)\rangle\right]\\
\nu_D &= \frac{1}{2}\langle(1-\epsilon)^2\theta_s^2\rangle,\\
\nu_\parallel &= \frac{1}{2}\langle\epsilon^2 + \theta_s^2\epsilon(1-\epsilon)\rangle.
\end{aligned} \tag{2.23}$$

Since the Fokker-Planck operator was obtained in the first place as a second-order expansion in $\Delta\mathbf{p}$, we can consistently neglect terms which are cubic or higher in ϵ and θ_s, which finally yields the general Fokker-Planck coefficients for an arbitrary binary interaction with stationary

targets (elastic as well as inelastic),

$$\begin{aligned}\nu_s &= \frac{1}{p}\langle p - p_1\rangle + \frac{1}{2p^2}\frac{\partial}{\partial p}\Big[p\langle (p-p_1)^2\rangle\Big],\\ \nu_D &= \langle 1-\cos\theta_s\rangle, \qquad (2.24)\\ \nu_\parallel &= \frac{1}{2p^2}\langle (p-p_1)^2\rangle. \qquad (2.25)\end{aligned}$$

We discover that the parallel diffusion frequency $\nu_\parallel$ is a higher-order term in the expansion than ν_s and will therefore tend to be negligible, since the validity of the equation requires small momentum transfers to dominate. In that case, we may approximate $\langle (p-p_1)^2\rangle \approx 0$. At highly relativistic speeds, we then see that $\nu_s = \langle p - p_1\rangle/p \approx \langle \gamma - \gamma_1\rangle m_e c^2/(vp)$ with a relative error of order $1/\gamma^2$. In that case, the dynamical friction F is given by

$$F = p\nu_s = \frac{1}{v}\langle m_e c^2(\gamma-\gamma_1)\rangle = n\int \mathrm{d}\sigma\, m_e c^2(\gamma-\gamma_1) \equiv -\left.\frac{\partial E}{\partial x}\right|_{\text{stopping}}$$

equalling the stopping power of the interaction. In fact, with this form of ν_s, the energy moment of the Fokker-Planck operator coincides exactly with that of the original Boltzmann operator even for non-relativistic speeds, as well as having the exact transport cross section (i.e. the $(1-\cos\theta)$-moment) thanks to the form of ν_D. We therefore propose the following Fokker-Planck coefficients to describe binary interactions with stationary targets which are dominated by small momentum transfers:

$$\begin{aligned}\nu_s &= \frac{m_e c^2}{vp}\langle \gamma - \gamma_1\rangle,\\ \nu_D &= \langle 1-\cos\theta_s\rangle, \qquad (2.26)\\ \nu_\parallel &= 0.\end{aligned}$$

Note that this model is only meant to describe the dynamics of the already-generated runaway electrons; to describe the generation of the seed population, in particular Dreicer generation, the non-vanishing speeds of the thermal population must be kept, which will lead (among other things) to a non-negligible energy-diffusion coefficient.

2.4 Effects of screening on the collision operator

Using the general Fokker-Planck equation derived in the previous section, given by Eqs. (2.19) and (2.26), we will now describe the collision

model that we propose in Paper E to model collisions between fast electrons and partially ionized ions. This requires us to calculate the collision frequencies ν_D and ν_s; unlike the regular Landau-Fokker-Planck equation where these are evaluated for a pure Coulomb interaction, they must now account for the screening effect of the bound electrons as well as the effect of ionizing collisions.

The determination of the slowing-down frequency ν_s is in practice the simpler task, as it only requires knowledge of the collisional stopping power. This is well known for an electron passing through a medium, and is described by the Bethe formula [71], yielding

$$\nu_s = \frac{e^4}{4\pi\varepsilon_0^2 m_e c^2}\frac{c^2}{pv^2}\sum_j n_j\left[Z_{0j}\ln\Lambda + N_{ej}\left(\ln\frac{cp\sqrt{\gamma-1}}{I_j} - \frac{v^2}{c^2}\right)\right]. \quad (2.27)$$

Here, the sum is taken over all ion species j (where different charge states are considered different species), Z_j denotes the atomic number, Z_{0j} the charge number (i.e. the net charge of the ion) and $N_{ej} = Z_j - Z_{0j}$ the number of bound electrons. Then, the slowing-down frequency is completely determined for any ion species j in terms of the three parameters Z_j, Z_{0j} and the mean-excitation energy I_j, which must be determined experimentally or by comprehensive atomic simulations. In our work we have used tabulated values from Sauer *et al.* [72] which have been given for all ionization degrees of some ion species, including the experimentally relevant argon and neon. The first term of the sum in Eq. (2.27) represents the contribution to the slowing-down frequency from elastic collisions with the free electrons, which can be treated as usual with the ideal theory yielding the familiar Coulomb logarithm $\ln\Lambda$.

In the determination of the deflection frequency ν_D, contributions will be obtained both from elastic collisions with the ion where its internal state does not change (which do not contribute significantly to ν_s since $\gamma - \gamma_1$ in such reactions is of the order of the mass ratio $m_e/m_i \ll 1$) as well as the inelastic collisions where the bound electrons are excited or ionized. In this case the elastic collisions provide the dominant contribution to ν_D, since the associated cross-section is of the order of $Z_j^2 r_0^2$. Conversely, the inelastic collisions – consisting mainly of incoherent interactions with individual bound electrons – scale as $(Z_j - Z_{0j})r_0^2$, and also tend to be more strongly peaked in the forward direction than the elastic collisions [73]. Therefore, for the highly charged ion species ($Z_j \gg 1$) in which we are primarily interested, such as neon and argon, the contribution is obtained by evaluating $\langle 1 - \cos\theta\rangle$ using only the dominant

elastic scattering cross-section.

In the Born approximation, the elastic differential cross section is given by

$$\mathrm{d}\sigma_j = \left|Z_j - F_j(\mathbf{p}_1 - \mathbf{p})\right|^2 \mathrm{d}\sigma_0, \tag{2.28}$$

where $\mathrm{d}\sigma_0$ is the electron-proton differential cross-section, given in the lab-frame by [62]

$$\frac{\partial\sigma_0}{\partial\cos\theta} = \frac{\pi r_0^2}{2(p/m_e c)^4}\frac{1+(p/m_e c)^2\cos^2(\theta/2)}{\sin^4(\theta/2)}. \tag{2.29}$$

The *atomic form factor* F_j, which completely describes the screening effect of the bound electrons, is given by

$$F_j(\mathbf{p}_1 - \mathbf{p}) = \int n_j(\mathbf{x}) \exp\left[\frac{i}{\hbar}\mathbf{x}\cdot(\mathbf{p}_1 - \mathbf{p})\right] \mathrm{d}\mathbf{x}, \tag{2.30}$$

where $n_j(\mathbf{x})$ is the number density of the bound electrons of ion species j, normalized such that $\int n_j(\mathbf{x})\,\mathrm{d}\mathbf{x} = N_{ej} = Z_j - Z_{0j}$ is the number of bound electrons, and the integration is taken over all space. For a spherically symmetric bound-electron density $n_j = n_j(r)$, it is found that the form factor only depends on the magnitude $q = |\mathbf{p}_1 - \mathbf{p}| = 2p\sin(\theta_s/2)$ of the momentum transfer;

$$F_j(q) = \frac{4\pi}{q}\int_0^\infty \mathrm{d}r\, r n_j(r)\sin qr. \tag{2.31}$$

The contribution to the deflection frequency from a single ion species is then given by

$$\begin{aligned}\nu_{Dj} &= 2n_j v \int \mathrm{d}\sigma_0 \sin^2\frac{\theta_s}{2}|Z_j - F_j(q)|^2 \\ &= 4\pi r_0^2 n_j c\frac{\gamma}{(p/m_e c)^3}\int_{1/\Lambda}^1 \mathrm{d}x\,\frac{1-x^2v^2/c^2}{x}|Z_j - F_j(2px)|^2,\end{aligned} \tag{2.32}$$

where $x = \sin(\theta_s/2)$, and the integral is taken from the minimum scattering angle $\theta_{s,\min} = 2/\Lambda \ll 1$ corresponding to Debye-length interaction distances. In Paper E, we show that in the high-energy limit $p \gg \hbar/a_0$ where a_0 is the Bohr radius (i.e. approximately the size of the ion), the diffusion coefficient takes the explicit form

$$\nu_D = \frac{4\pi c r_0^2\gamma}{(p/m_e c)^3}\sum_j n_j\left[Z_j^2\ln\Lambda + (Z_j^2 - Z_{0j}^2)\ln\left(\frac{pa_j}{\hbar}\right) - \frac{2}{3}(Z_j - Z_{0j})^2\right], \tag{2.33}$$

where the ion properties are again completely captured by three parameters Z_j, Z_{0j} as well as the new parameter a_j which defines an effective ion radius given by an integral over the bound-electron density $n_j(r)$. In Paper E we have tabulated values for a_j for He, Be, C, N, Ne, Ar, Xe and W, where n_j was determined through density-functional-theoretical calculations using the tools EXCITING [74] and GAUSSIAN [75]. To give an indication of the magnitude of the effective ion radii, a few explicit values normalized to the Bohr radius as produced by the simulations are: $a_j/a_0 \approx 0.81$ for neutral neon Ne; 0.70 for neutral argon Ar; and 0.32 for Ar^{+9}.

From the above expressions for ν_s and ν_D, we find that the modifications to the Fokker-Planck coefficients are sensitive to the runaway energy. In the low-energy limit, the completely screened situation is retrieved where the electrons only sense the net charge of the ions; however, significant departures are demonstrated already at runaway energies exceeding 100 eV. For characteristic runaway energies in the 10 MeV range, and for high-Z impurities of low ionization degree, the pitch-angle deflection rate is typically reduced to approximately 60% of its non-screened value, and the dynamical friction typically by 20-30%. At lower energies of ~ 1 MeV, the screening effect tends to be of the order of 70% and 50% for deflection and friction, respectively.

2.5 CODE

An approximate Fokker-Planck collision operator to study runaway electrons was developed in Ref. [76]. It is an asymptotic matching of the linearized Beliaev-Budker operator (2.18) in the high-energy limit with the non-relativistic collision operator [58, 77] (corresponding to Eq. (2.18) for $v \ll c$, linearized with a cold bulk of thermal velocity $v_{Te} = \sqrt{2T_e/m_e} \ll c$). The operator is, in terms of Eq. (2.19), given by

$$
\begin{aligned}
A(p) &= \frac{m_e^2 c^2}{\tau_c} \frac{c}{vp} G\left(\frac{v}{v_{Te}}\right), \\
\nu_s(p) &= \frac{2}{p} \frac{m_e c}{\tau_c} \frac{c^2}{v_{Te}^2} G\left(\frac{v}{v_{Te}}\right), \\
\nu_D(p) &= \frac{m_e^2 c^2}{\tau_c} \frac{c}{v} \left[Z_{\text{eff}} + \phi\left(\frac{v}{v_{Te}}\right) - G\left(\frac{v}{v_{Te}}\right) + \frac{1}{2} \frac{v_{Te}^2}{c^2} \frac{v^2}{c^2} \right].
\end{aligned}
$$

Here we have introduced the error function $\phi(x) = 2\pi^{-1/2} \int_0^x \mathrm{d}s \, \exp(-s^2)$ and the Chandrasekhar function $G(x) = (\phi(x) - x\phi'(x))/2x^2$. A term

proportional to the plasma effective charge $Z_{\text{eff}} = \sum_i n_i Z_i^2 / n_e$ (the sum taken over all ion species in the plasma) has been added to the pitch-angle scattering operator coefficient, which corresponds to the contribution from ions in the plasma, taken to be stationary. This collision operator was implemented in the numerical tool CODE [78], with more recent improvements to the model described in Paper L. CODE obtains solutions to the kinetic equation (2.3) treated as an initial-value problem, but has been extended during this thesis with additional terms to describe the effect of synchrotron and bremsstrahlung losses as well as of large-angle collisions. By representing the distribution function in terms of Legendre polynomials in pitch-angle cosine and a finite-difference discretization of the momentum coordinate, a flexible and computationally efficient scheme is obtained. The model contains the essential physics needed in order to study a wide range of momentum-space runaway dynamics, making it highly suited for studies such as those presented in this thesis.

A separate numerical tool, NORSE (NOn-linear Relativistic Solver for Electrons), has also been developed which solves the electron kinetic equation using the full non-linear relativistic Fokker-Planck equation (2.18). The tool is presented in Paper N, and is also freely available to download[1]. The method must be used whenever the deviations from a local Maxwellian distribution are large; this may for example be the case when the runaway population is comparable in number to the thermal population, or when the thermal energy of the distribution varies on a time-scale comparable to the collision time. The latter may be important during the thermal-quench phase of a disruption, and non-linear effects could plausibly have an influence on hot-tail runaway generation. A case study of the former situation was analyzed in Paper M, where NORSE was applied to investigate slide-away runaway generation in a post-disruption plasma.

[1] Original published version available at `http://doi.org/10.17632/86wmgj758w.1`, with an updated version at `https://github.com/hoppe93/NORSE`.

Chapter 3

Radiation emitted by runaway electrons

Radiation is essential in order to understand electron runaway. When electrons emit radiation, they transfer a fraction of their kinetic energy to the electromagnetic field. This affects their phase-space dynamics, and radiation losses can for example limit the maximum energy achievable in a given accelerating electric field, where the dominant energy-loss channels are through synchrotron radiation as well as bremsstrahlung. In the classical theory of radiation reaction [79, 80, 81], it is assumed that a charged particle undergoes smooth accelerated motion. Maxwell's equations for a point source then yields the rate at which momentum is gained by the electromagnetic field; by imposing the conservation of momentum, this yields an associated average radiation reaction force experienced by the particle which is given by the Abraham-Lorentz-Dirac force

$$\mathbf{F}_{\mathrm{ALD}} = \frac{e^2\gamma^2}{6\pi\varepsilon c^3}\left[\dot{\mathbf{v}} + \frac{3\gamma^2}{c^2}(\mathbf{v}\cdot\dot{\mathbf{v}})\dot{\mathbf{v}} + \frac{\gamma^2}{c^2}\left(\mathbf{v}\cdot\ddot{\mathbf{v}} + \frac{3\gamma^2}{c^2}(\mathbf{v}\cdot\dot{\mathbf{v}})^2\right)\mathbf{v}\right]. \quad (3.1)$$

For runaways in magnetized plasmas, this force tends to be dominated by the synchrotron radiation reaction due to the rapid gyration of the electrons at the cyclotron frequency $\Omega_B = eB/(\gamma m_e)$ [82]. The effects on runaways of including the synchrotron-reaction force in the kinetic equation is explored in-depth in Papers G, H, I and K. In particular, Paper I includes the full guiding-center transformation to first order of the ALD force for energetic electrons in magnetized plasmas.

Radiation is also one of few ways in which a runaway beam can be passively diagnosed, since it is typically emitted at such short wave-

lengths that the plasma is optically thin to this radiation; particularly in tokamaks is this generally the case. Observation of the emission provides insight into the runaway distribution function, which allows the validity of runaway models to be assessed.

3.1 Bremsstrahlung radiation reaction

When charged particles collide, the resulting emission is referred to as *bremsstrahlung* (German for "braking radiation", as it causes the particles to decelerate) [83, 84]. Unlike synchrotron radiation, as discussed above, the bremsstrahlung emission is not emitted due to smooth macroscopic motion, but rather in bursts during the brief microscopic interactions of runaways colliding with the background plasma. As such, a statistical approach can be taken where we consider only the *total momentum* $\mathbf{k}$ lost to the electromagnetic field in each collision (in the classical picture corresponding to the time-integrated radiation reaction force), and consider the differential cross-section $\partial\sigma_{\mathrm{br},j}/\partial\mathbf{p}$ for runaways of momentum $\mathbf{p}_1$ incident on a target of species j to end up with momentum $\mathbf{p}$ after the collision. Then, since the microscopic interactions are dominated by binary collisions, the bremsstrahlung radiation reaction is governed by a Boltzmann collision operator of the form given in Eq. (2.5), which for stationary targets is given by

$$C_{\mathrm{br}} = \sum_j n_j \int \mathrm{d}\mathbf{p}_1\, v_1 f_e(\mathbf{p}_1) \frac{\partial\sigma_{\mathrm{br},j}(\mathbf{p};\,\mathbf{p}_1)}{\partial\mathbf{p}} - v f_e(\mathbf{p}) \sum_j n_j \sigma_{\mathrm{br},j}(\mathbf{p}). \tag{3.2}$$

In the classical theory of bremsstrahlung one finds that the frequency ω of the bremsstrahlung radiation becomes large enough that the total energy $c|\mathbf{k}|$ emitted in individual collisions becomes comparable to the photon energy $\hbar\omega$ [83]. Hence the classical theory breaks down, and only quantum theory can describe the bremsstrahlung process. The differential cross-section $\partial\sigma_{\mathrm{br},j}/\partial\mathbf{p}$ was given for interactions with stationary ions in the Born approximation in Refs. [85, 86]. From the differential cross-section it is found that relativistic electrons on average lose a significant fraction of their kinetic energy in each bremsstrahlung emission, indicating that a Fokker-Planck equation for bremsstrahlung losses is inadequate. We reproduce the dominant single-photon bremsstrahlung

differential cross section given in Ref. [86], which can be written as

$$\frac{\partial\bar{\sigma}_{ab}}{\partial\mathbf{p}} = Z_b^2\alpha r_0^2\frac{2k}{p_1\gamma}W(p;\,p_1,\,\cos\theta_s)$$

$$\begin{aligned}
W(p;\,p_1,\,\cos\theta_s) = {} & \frac{2\gamma_1\gamma+(\gamma_1^2+\gamma^2-1)\lambda-\lambda^2}{k^2\lambda^2\sqrt{\lambda(\lambda+2)}}\ln\left(1+\lambda+\sqrt{\lambda(\lambda+2)}\right)\\
& -\frac{2\gamma_1\gamma-\lambda}{k^2\lambda^2}-\frac{3(\gamma_1^2\gamma^2-1)^2}{\lambda^2p_1^4p^4}\\
& +\frac{4(\gamma_1^2\gamma^2-\gamma_1\gamma+1)-\gamma_1\gamma(p_1^2+p^2)+(\gamma_1^2+\gamma^2+\gamma_1\gamma-1)\lambda}{2\lambda^2p_1^2p^2}\\
& +\left(2\frac{\gamma_1\gamma-1}{\lambda^3}-\frac{k^2}{\lambda^4}\right)\frac{2(\gamma_1^2+\gamma^2-\gamma_1\gamma)p_1^2p^2+3k^2(\gamma_1+\gamma)^2}{p_1^4p^4}\\
& +\frac{l}{p^3}\left[\frac{\gamma+2\gamma^3}{\lambda^2p^2}+\frac{2\gamma^4+2p_1^2p^2+\gamma_1(\gamma_1+\gamma)-(\gamma_1\gamma+p^2)\lambda}{2k\lambda^2}\right.\\
& \left.+\gamma\left(2\frac{\gamma_1\gamma-1}{\lambda^3}-\frac{k^2}{\lambda^4}\right)\frac{2\gamma_1p^2-3k\gamma^2}{kp^2}\right]\\
& +\frac{l_1}{p_1^3}\left[\frac{\gamma_1+2\gamma_1^3}{\lambda^2p_1^2}-\frac{2\gamma_1^4+2p_1^2p^2+\gamma(\gamma_1+\gamma)-(\gamma_1\gamma+p_1^2)\lambda}{2k\lambda^2}\right.\\
& \left.-\gamma_1\left(2\frac{\gamma_1\gamma-1}{\lambda^3}-\frac{k^2}{\lambda^4}\right)\frac{2\gamma p_1^2+3k\gamma_1^2}{kp_1^2}\right]. \qquad (3.3)
\end{aligned}$$

In the expression for W, the electron momenta p_1 and p, and photon momentum k, have been normalized to m_ec for clarity. The fine-structure constant is denoted $\alpha = e^2/(4\pi\varepsilon_0\hbar c) \approx 1/137$, and $r_0 = e^2/(4\pi\varepsilon_0 m_ec^2) \approx 2.8\cdot10^{-15}$ m is again the classical electron radius. We have also introduced the auxiliary quantities

$$\begin{aligned}
l &= \ln(\gamma+p),\\
l_1 &= \ln(\gamma_1+p_1),\\
\lambda &= \gamma_1\gamma - p_1p\cos\theta_s - 1,
\end{aligned}$$

where the full angular dependence of the cross-section is captured in λ.

In the context of runaway in magnetic-fusion plasmas, the effects of bremsstrahlung losses have been studied within the approximation that runaways experience only the mean force [87, 88, 89]

$$\mathbf{F}_{\rm br}(\mathbf{p}) = -\hat{v}\sum_j n_jc\int_0^{\gamma-1}(kc)\frac{\partial\sigma_{{\rm br},j}}{\partial k}{\rm d}k, \qquad (3.4)$$

where $\partial\sigma_{\mathrm{br},j}/\partial k$ is the cross-section for a photon of energy k to be emitted, and describes the average energy loss in the sense that

$$\int \mathrm{d}\mathbf{p}\, m_e c^2(\gamma-1)C_{\mathrm{br}}(\mathbf{p}) = \int \mathbf{v}\cdot\mathbf{F}_{\mathrm{br}}(\mathbf{p}) f_e(\mathbf{p})\,\mathrm{d}\mathbf{p}. \tag{3.5}$$

The model is equivalent to using the Fokker-Planck operator (2.19) with coefficients (2.26) to describe the bremsstrahlung reaction, taking $\nu_D = 0$. In these studies it was found that bremsstrahlung emission could play an important role in limiting the maximum achievable energy for a runaway being accelerated in an electric field near the threshold value E_c. It was found to be particularly important for high plasma charge Z [88], and also that its relative importance compared to synchrotron loss increases with density [87]. It was concluded that in a range of typical tokamak disruption scenarios, bremsstrahlung losses would play an important role in limiting the runaway kinetic energy.

In Paper B, we extend the model used in previous studies of bremsstrahlung emission during electron runaway to utilize the full statistical description of Eq. (3.2) for the bremsstrahlung energy loss. In the mean-force picture of the previous studies, for a given accelerating electric field there will be a well-defined kinetic energy above which the bremsstrahlung radiation loss will exceed the force due to the electric field, thus setting a sharp upper boundary for the runaway energy. Conversely, in the statistical description there is a non-zero probability that a runaway will be accelerated for an arbitrarily long time before emitting a photon in a bremsstrahlung reaction. One could thus expect that the energy distribution of runaways exhibits a tail that extends beyond the critical energy where the *average* energy loss balances the electric field. Indeed, this behavior was found in Paper B from numerical solutions of the kinetic equation; a main result of the study is that in the statistical model using a Boltzmann operator, approximately 10% of the total runaway kinetic energy in steady state is carried by electrons with energy at least 80% higher than the theoretical prediction in the mean-force model.

Paper B also explores the pitch-angle deflection of fast electrons during bremsstrahlung emission. In the study, we found that this effect can generally be neglected for those reactions where the photon energy is comparable to the electron energy, which are responsible for the majority of the total energy loss. However, the contribution to pitch-angle scattering is found to increase rapidly as the photon energy approaches zero, and the total bremsstrahlung-assisted pitch angle scattering rate can become significant compared to ordinary (elastic) collisional pitch

angle scattering for fast electrons with energy in the GeV range. For runaways, which are generally in the 10-100 MeV energy range, the effect tends to be minor.

3.2 Synthetic radiation diagnostic

On the other side of the coin is the question of the characteristics of the emitted radiation. Interpreting the synchrotron and bremsstrahlung radiation emitted by a plasma containing runaways is the most promising method of probing the runaway phase-space distribution. For example, in contrast, the runaway current depends only on the average runaway velocity, which tends to be at the speed of light aligned with the magnetic field, and is largely insensitive to the runaway energies. Inferring the runaway distribution from the emitted radiation is complicated by the fact that only line-integrated measurements can be performed, and that different combinations of energy and pitch can often produce relatively similar emission. This can be particularly challenging when only parts of the spectrum are measured, such as when using a camera sensitive to emission in the visible range to detect synchrotron emission which tends to be the strongest in the infra-red range during runaway in tokamaks.

There are many examples in the literature of runaway distributions that have been inferred from experimental observations of radiation emitted in plasmas where runaway acceleration was believed to occur. In Refs. [90, 91] the bremsstrahlung emission of a runaway beam was observed in the DIII-D tokamak with temporal, angular and spectral resolution. From these measurements, imposing a set of simplifying assumptions, runaway energy spectra were reconstructed which were qualitatively consistent with a runaway model similar to the ones employed in this thesis. The energy reconstruction reveals an anomaly, however, where the experimentally observed runaways appear to have significantly lower maximum energies than can be understood in a spatially-homogeneous description. This finding is consistent with other reconstructions that have been made, such as in Ref. [92] where a reconstruction was performed using combined radiation diagnostics in a DIII-D post-disruption plasma. Recent analysis of camera images in the EAST tokamak, which are assumed to show the synchrotron emission of runaways due to the asymmetric pattern, has been used to infer the radial distribution of the runaway population, as well as its characteristic energy and pitch [93].

We shall now introduce a synthetic diagnostics method which predicts the emission that a detector would observe due to a runaway population in tokamaks. Formally, the spectral radiance (dimension $\mathrm{W}/(\mathrm{m}^2\,\mathrm{st}\,\mathrm{Hz})$) reaching a detector placed at a location $\mathbf{x}_0$; facing a direction $\mathbf{n}_0$; along the line-of-sight described by a unit vector $\mathbf{n}$ and parametrized by a solid angle Ω_n; and at a frequency ω, can for an optically thin plasma be written in terms of the received power P as [94]

$$\frac{\partial P}{\partial A \partial \Omega_n \partial \omega} = \int \mathrm{d}\mathbf{x}\mathrm{d}\mathbf{p}\, \frac{\mathbf{n}\cdot\mathbf{n}_0}{|\mathbf{x}-\mathbf{x}_0|^2}\delta\left(\frac{\mathbf{x}-\mathbf{x}_0}{|\mathbf{x}-\mathbf{x}_0|}-\mathbf{n}\right)\frac{\partial P(\mathbf{x},\mathbf{p},\mathbf{n})}{\partial\Omega\partial\omega} f_e(\mathbf{x},\mathbf{p}), \tag{3.6}$$

where $\partial P/\partial\Omega\partial\omega$ is the differential received power due to a fast electron at the location $(\mathbf{x},\mathbf{p})$.

In Paper F, the synthetic diagnostic SOFT (Synchrotron-detecting Orbit Following Toolkit) is presented which evaluates this integral with $\partial P/\partial\Omega\partial\omega$ appropriately chosen to describe synchrotron radiation, which has later been generalized to also allow bremsstrahlung emission to be modeled (Paper P). The method is specialized to magnetized toroidal systems that vary on a time-scale much longer than the transit time scale ($\tau \gg L/c \sim 10\,\mathrm{ns}$ for runaways, where L indicates the system dimension). In that case, the distribution function can be fully described in terms of one spatial coordinate and two momentum coordinates. The dependence on one momentum coordinate, the gyroangle, vanishes in a magnetized plasma due to the rapid gyromotion; one spatial coordinate vanishes due to Liouville's theorem stating that for Hamiltonian motion the distribution function is constant along phase-space particle trajectories; and the final spatial coordinate, the toroidal angle, vanishes by the assumed symmetry. The resulting integral can be written

$$\frac{\partial P}{\partial A \partial \Omega_n \partial \omega} = \int \mathrm{d}x_1\mathrm{d}p_1\mathrm{d}p_2\, f_e(x_1,p_1,p_2)K(x_1,p_1,p_2;\,\mathbf{x}_0,\mathbf{n}_0,\mathbf{n},\omega), \tag{3.7}$$

where x_1, p_1 and p_2 are suitable guiding-center phase space coordinates describing the distribution function f_e; the kernel function K, which SOFT calculates, provides a complete description of the emission that a detector can observe from any runaway population.

Additional insight into the observed emission from runaways can be gained by noting that for high energies, due to the relativistic-beaming effect, the emission is narrowly focused along the particle direction of

motion, and one obtains

$$\frac{\partial P}{\partial \Omega \partial \omega} \to \delta\left(\frac{\mathbf{p}}{p} + \mathbf{n}\right) \frac{\partial P}{\partial \omega}. \tag{3.8}$$

When this expression is averaged over the electron gyroangle φ, one obtains

$$\frac{1}{2\pi}\int_0^{2\pi} \mathrm{d}\varphi \frac{\partial P}{\partial \Omega \partial \omega} = \delta\left(\cos\theta - \hat{V}\cdot\mathbf{n}\right)\frac{\partial P}{\partial \omega}, \tag{3.9}$$

where $\hat{V}$ is the unit vector representing the guiding-center direction of motion. This means that emission can only be detected while the condition

$$\cos\theta = \hat{V}\cdot\mathbf{n} = \hat{V}(\mathbf{B}(\mathbf{x}), \nabla\mathbf{B}(\mathbf{x}), p, \theta)\cdot\frac{\mathbf{x}-\mathbf{x}_0}{|\mathbf{x}-\mathbf{x}_0|} \tag{3.10}$$

is satisfied, where the guiding-center velocity $\mathbf{V}$ depends on the local magnetic field (and its gradients) and the electron momentum. Due to the conservation of magnetic moment along trajectories, the pitch-angle $\theta = \theta(\mathbf{x})$ will also be a function of location. The solution of this equation for $\mathbf{x}$ – given a magnetic field, detector location, particle energy and magnetic moment – represents a two-dimensional surface which we refer to as the *surface-of-visibility* (SoV); only when runaways cross this surface will they contribute observable emission, and so the SoV can explain roughly the shape of synchrotron emission spots observed by cameras in tokamaks. These synchrotron spot shapes have been previously studied in Ref. [93], using a method outlined in Ref. [95] to obtain them.

Within the observed spot, we can identify two main effects which determine the intensity variations:

(i) The variation of the emitted intensity $\partial P/\partial\omega$ across the plasma. For synchrotron radiation this depends strongly on the local magnetic-field strength, which is approximately inversely proportional to the major radius. This generally causes enhanced observed emission from the high-field-side of the device. For detectors which only observe the low-frequency tail of the emitted spectrum, this effect is so strong that the observed spot shape is completely altered.

(ii) The geometrical effect, by which we mean the combination of the geometry of the magnetic field (or of the runaway trajectories), of the detector (location and shape) and of the angular distribution of

radiation. These have an effect that can be understood in terms of the *time along the runaway trajectory* that the surface-of-visibility condition is satisfied for a finite-extent camera. This can vary dramatically across the spot, and often takes a sharp maximum along the edge of the SoV (where runaways move tangentially to the surface) where orders-of-magnitude stronger detected intensities may be observed.

In particular the geometrical effect has been out of reach of previous studies of the synchrotron emission from runaways – which considered mainly spot shapes or total emission [96] – but is demonstrated to be essential in order to understand runaway images. It must, however, be stressed that the SoV is strongly dependent on the runaway momentum (especially the pitch angle, which enters explicitly into the SoV equation), and hence a complete image resulting from a distribution of runaways would be the superposition of contributions from various different surfaces-of-visibility. This reveals patterns that are often not evident from studying individual SoVs, thereby illustrating that a complete synthetic-diagnostic simulation (using e.g. SOFT) is generally required in order to predict the observed pattern.

Chapter 4

Runaway of positively charged species

In previous chapters of this thesis we have focused on electron runaway. In Papers C and D, however, we consider the runaway of positively charged particle species in plasmas. Although the fundamental runaway mechanism is shared with electrons, being essentially a competition between the accelerating force and collisional friction, there are differences which alter the picture.

4.1 Positron runaway

In Paper C we consider the runaway of positrons. These are typically generated during runaway scenarios by interactions between the thermal background plasma and the ultra-relativistic runaway electrons [97], whose energies in the 10-100 MeV range far exceed the pair-production threshold of $2m_ec^2 \approx 1\,\mathrm{MeV}$. The defining feature of positron runaway, which sets it apart from regular electron runaway, is not their annihilation – which often occurs on time-scales longer than the runaway discharge lasts – but rather that they tend to be created moving in the direction opposite to that of their acceleration. Positrons produced in collisions of ultra-relativistic runaways will tend to be co-moving with the incident electrons, which are in turn moving predominantly antiparallel to the electric field due to their negative charge. Consequently, newly created pairs are moving antiparallel to the electric field, but the positrons will be accelerated along the field. This means that they will initially be slowed down by the electric field, and only a fraction will have

scattered to sufficiently large momenta perpendicular to the electric field that they will not thermalize before reaching the runaway region.

A common feature of many of the studies presented in this thesis is the role of large-angle collisions, and positron runaway is no exception. The creation of positrons in collisions between runaways and background ions is again given by a form of Eq. (2.5):

$$S_{\mathrm{pos}}(\mathbf{p}) = \sum_j n_j \int \mathrm{d}\mathbf{p}_1 \, v_1 f_e(\mathbf{p}_1) \frac{\partial \sigma_{\mathrm{pos,j}}(\mathbf{p};\, \mathbf{p}_1)}{\partial \mathbf{p}}, \tag{4.1}$$

which describes the rate of creation of positrons at momentum $\mathbf{p}$, where $\sigma_{\mathrm{pos,j}}$ is the cross-section for positron generation in the interaction between a runaway electron of momentum $\mathbf{p}_1$ and a stationary target particle of species j. Note that the term depends only on the runaway-electron population, and not the positron distribution itself. For highly energetic electrons $p_1 \gg m_e c$, the cross section is sharply peaked for $\mathbf{p}$ parallel to $\mathbf{p}_1$, and one may approximate

$$\frac{\partial \sigma_{\mathrm{pos,j}}(\mathbf{p};\, \mathbf{p}_1)}{\partial \mathbf{p}} = \frac{\delta\left(1 - \frac{\mathbf{p}_1 \cdot \mathbf{p}}{p_1 p}\right)}{2\pi p \gamma m_e^2 c^2} \frac{\partial \sigma_{\mathrm{pos,j}}(p, p_1)}{\partial \gamma}, \tag{4.2}$$

where the problem is reduced to finding the cross-section differential in the outgoing positron energies $\partial \sigma_{\mathrm{pos,j}}(p, p_1)/\partial \gamma$. However, with collisional pair production being a second-order process in quantum electrodynamics, no closed-form expressions for the cross-section are available in the published literature to the author's knowledge. Instead, we have opted to use the numerical tool MadGraph 5 [98] to provide the differential cross sections. We point out that a numerically-fitted total cross-section formula given by Gryaznykh [99] – which has been used in a number of previous studies of positron runaway – disagrees with the MadGraph 5 calculation by a nearly constant factor of four. Since the MadGraph output agrees with the analytical high-energy limit given in Appendix F of Ref. [100] within 5% for all electron energies above 100 MeV, we deem it likely that there is an error in the calculation of Ref. [99]. Consequently, previous studies have overestimated the collisional pair production of positrons by approximately a factor of four.

The annihilation of positrons, on the other hand, is given by

$$S_{\mathrm{an}}(\mathbf{p}) = -v f_{\mathrm{pos}}(\mathbf{p}) \sigma_{\mathrm{an}}(\mathbf{p}) \tag{4.3}$$

where σ_{an} is the total annihilation cross section for a positron of momentum $\mathbf{p}$. In a fully ionized plasma, it is given by the free-free two-quanta annihilation cross section [62]

$$\sigma(\mathbf{p}) = \frac{\pi r_0^2}{\gamma+1}\left[\frac{\gamma^2+4\gamma+1}{\gamma^2-1}\ln(\gamma+\sqrt{\gamma^2-1}) - \frac{\gamma+3}{\sqrt{\gamma^2-1}}\right]. \qquad (4.4)$$

For positron energies much greater than the rest energy, $\gamma \gg 1$, it is a decreasing function of energy $\sigma_{\text{an}} \sim \pi r_0^2(\ln 2\gamma - 1)/\gamma$, hence the mean life time $1/(nc\sigma_{\text{an}})$ tends to be much longer than for example the avalanche time which is of the order of $[2\pi n r_0^2 c(E/E_c - 1)]^{-1}$.

In Paper C, we discovered that the fraction of created positrons that end up running away is highly sensitive to the electric-field strength, but relatively insensitive to the plasma charge. For example, at $E = 2E_c$ the runaway fraction was approximately 20%, whereas at $10E_c$ it reaches 60-80%. We also analyzed the possibility to measure the annihilation radiation that is emitted by the positrons that are slowed down instead of becoming runaway accelerated. Since this emission is strongly peaked around the distinct photon energy of 511 keV, there is hope that this annihilation radiation can be distinguished from the X-ray emission from the runaway electrons. We found that a fine energy resolution is required from a HXR spectrometer for this to be possible: if a peak in the photon-energy spectrum narrower than 1 keV can be resolved, it could be feasible to observe the runaway-created positrons in an ideal scenario. If this resolution requirement is not met, coincidence-measurement techniques may be employed to improve the signal-to-noise ratio [101].

4.2 Ion runaway

In Paper D we have studied the runaway of ion species present in the plasma. The defining feature here is the large mass of the runaway ions, where even strongly superthermal ions tend to be slower than the thermal electrons. The result is a dynamical friction force which does not decrease monotonically for speeds above the thermal, but instead grows as the ion speed approaches the thermal electron speed. This leads to runaway ions not actually running away; they will instead be accelerated towards some equilibrium speed. However, since the generation of these superthermal ions by strong electric fields is very similar to the electron runaway process, they are referred to as runaway ions.

The presence of a much lighter species in the plasma – the electrons – sets the ion runaway process apart from electron and positron runaway. The kinetic equation for an ion species i is given by

$$\frac{\partial f_i}{\partial t} + \frac{eZ_i}{m_i} E_\parallel \frac{\partial f_i}{\partial v_\parallel} = C_{ie} + \sum_j C_{ij}, \tag{4.5}$$

where the sum is taken over all ion species present in the plasma. The ion-electron collision operator can be written

$$C_{ie} = C_{ie}[f_i, f_e] = C_{ie}[f_i, f_{Me}] + C_{ie}[f_i, f_e - f_{Me}], \tag{4.6}$$

where we take f_{Me} to be a Maxwellian electron distribution in the rest-frame of the ion population. During near-equilibrium scenarios, i.e. when $E \ll E_D$, the perturbed electron population $f_e - f_{Me}$ only contributes significantly from electron speeds much greater than the characteristic runaway ion speeds. Since the first term $C_{ie}[f_i, f_{Me}]$ produces no net momentum transfer for the chosen f_{Me}, the operator can then be written [70]

$$C_{ie}[f_i, f_e - f_{Me}] = \frac{\mathbf{R}_{ei}}{m_i n_i} \cdot \frac{\partial f_i}{\partial \mathbf{v}}, \tag{4.7}$$

where $\mathbf{R}_{ei} = \int \mathrm{d}\mathbf{v}\, m_e \mathbf{v} C_{ei}$ is the net electron-ion friction force. The ion-electron friction $\mathbf{R}_{ie}$ is readily calculated from the electron momentum equation,

$$\frac{\partial (n_e m_e \mathbf{V}_e)}{\partial t} = -n_e e \mathbf{E} + \sum_j \mathbf{R}_{ej}. \tag{4.8}$$

In steady state, utilizing that electron-ion collision rates scale as the ion-charge squared, we obtain

$$n_e e \mathbf{E} = \sum_j \mathbf{R}_{ej} = \frac{n_e Z_{\mathrm{eff}}}{n_i Z_i^2} \mathbf{R}_{ei}, \tag{4.9}$$

where the effective charge is defined by $\sum_i n_i Z_i^2 = n_e Z_{\mathrm{eff}}$. This allows the collisions with the perturbed electron population to be combined with the electric field to yield an ion kinetic equation

$$\begin{aligned} \frac{\partial f_i}{\partial t} + \frac{eZ_i}{m_i} E_\parallel^* \frac{\partial f_i}{\partial v_\parallel} &= C_{ie}[f_i, f_{Me}] + \sum_j C_{ij}[f_i, f_j], \\ E_\parallel^* &= \left(1 - \frac{Z_i}{Z_{\mathrm{eff}}}\right) E_\parallel. \end{aligned} \tag{4.10}$$

In a pure plasma, where $Z_i = Z_{\text{eff}}$, the effective electric field $E_\parallel^*$ vanishes and no ion acceleration will occur. For a high-Z impurity with $Z_i \gg Z_{\text{eff}}$, the drag against electrons will far exceed the acceleration by the electric field, and the impurities will be accelerated in the direction of electron runaway, i.e. anti-parallel to the electric field.

For a runaway ion, the collisions with f_{Me} will describe a dynamical friction $F_{ie} \propto v$ increasing in proportion to speed up to the electron thermal speed, whereas the collisions with other ions result in a friction force $F_{ij} \propto 1/v^2$, as in the standard electron runaway situation.

We developed an open source numerical tool CODION [102], based on the runaway-electron solver CODE but accounting for the additional terms of the kinetic equation specific to ion runaway, which we used to study the ion runaway dynamics in Paper D.

Ion friction-force estimates

Valuable physical insight into the ion runaway process can be obtained by considering the friction force acting on a test-ion moving through the plasma. Formally, the test-particle equations of motion can be obtained by considering velocity moments of the kinetic equation for a delta distribution $f_a = \delta(\mathbf{v} - \mathbf{u}(t))$ representing the test particle [103]. This method was pursued in Refs. [39, 42] where ion runaway in solar flares was considered, and later expanded upon in Paper D to consider general plasma compositions. The momentum moment of the ion kinetic equation yields the test-particle equation of motion

$$\frac{\partial(m_i v)}{\partial t} = Z_i e E^* \xi - \frac{m_i v_{Ti}}{\tau_{ie}} \left(\frac{Z_{\text{eff}} + \bar{n}}{v^2/v_{Ti}^2} + \frac{4}{3\sqrt{\pi}} \sqrt{\frac{m_e T_i^3}{m_i T_e^3}} \frac{v}{v_{Ti}} \right),$$

where we use the pitch-angle cosine $\xi = v_\parallel/v$, the ion-electron collision frequency $\tau_{ie}^{-1} = n_e \ln\Lambda Z_i^2 e^4/(4\pi\epsilon_0^2 m_i^2 v_{Ti}^3)$, and introduced the quantity $\bar{n} = \sum_j n_j Z_j^2 m_j/(n_e m_i)$. Here explicit expressions for the collision operator with a Maxwellian background species [103] have been used, under the assumption that the velocities satisfy $v_{Tj} \ll v \ll v_{Te}$ for all ion species j. The term containing the parentheses represents collisional friction, in which the first term expresses ion-ion friction which decreases with velocity and dominates for low velocities, whereas the second term describing ion-electron friction increases with velocity and dominates at high velocities.

The solutions $\partial(m_i v)/\partial t = 0$ represent those velocities where electric-field acceleration exactly balances collisional friction. For electric fields

$$E^* > E^*_{\min} = 2\frac{m_i v_{Ti}}{Z_i e \tau_{ie}} \frac{T_i}{T_e} \left(\frac{3}{2\pi} \frac{m_e}{m_i} (Z_{\text{eff}} + \bar{n}) \right)^{1/3},$$

two solutions v_{c1} and v_{c2} exist which describe, respectively, the runaway velocity above which an ion will be accelerated by the electric field; and the maximum velocity before electron friction overcomes the electric field, thus preventing further acceleration. Therefore, ions with velocity $v_{c1} < v < v_{c2}$ will be accelerated, before accumulating at v_{c2}.

However, it should be noted that the above test-particle equation of motion is not unique. By considering the energy moment $\int \mathrm{d}\mathbf{v}\, m_i v^2/2(\ldots)$ of the ion kinetic equation, one instead obtains

$$\frac{\partial(m_i v)}{\partial t} = Z_i e E^* \xi - \frac{m_i v_{Ti}}{\tau_{ie}} \left[\bar{n} \frac{v_{Ti}^2}{v^2} + \frac{4}{3\sqrt{\pi}} \sqrt{\frac{m_e T_i^3}{m_i T_e^3}} \left(\frac{v}{v_{Ti}} - \frac{3T_e}{T_i} \frac{v_{Ti}}{v} \right) \right].$$

If we assume that $(v/v_{Ti})^2 \gg 3T_e/T_i$, this reduces to the momentum equation with the simple exchange $\bar{n} \mapsto Z_{\text{eff}} + \bar{n}$. This equation may provide more accurate estimates of the critical velocities; using the same procedure to estimate the electron runaway velocity shows that the energy-balance equation yields the well-known formula $v_c/v_{Te} = \sqrt{E_D/2E}$, while the momentum-balance equation gives a result which is larger by a factor $\sqrt{2}$. The discrepancy may be understood by the fact that pitch-angle scattering contributes to friction in the momentum-balance equation, but not in the energy-balance equation as it is an energy-conserving effect. The angular deflection will not efficiently stop a particle from running away (except sometimes indirectly), and hence the energy equation provides a better estimate. The substitution $(Z_{\text{eff}} + \bar{n}) \mapsto \bar{n}$ may thus improve the results given in Refs. [39, 42] and Paper D, although these estimates should perhaps primarily be viewed as a guide to interpret solutions of the kinetic equation, and to make qualitative predictions regarding the features of the ion runaway distribution.

Note finally the limits to the validity of the model described here. The linearization of the self-collision operator requires small runaway densities, corresponding to short times or electric fields $E^* \sim E^*_{\min}$; extending far above $E^*_{\min}$ requires the use of a non-linear self-collision operator. At the same time, the electric field must be sufficiently weak to avoid significant runaway-electron generation which would affect E^*, therefore requiring $E \lesssim 0.1 E_D$.

Chapter 5

Summary and outlook

Runaway is an important phenomenon, which occurs in both terrestrial and space plasmas. It is of particular interest in magnetic-fusion research where runaway electrons can strike the wall of the reactor after being accelerated to highly relativistic energies, at which point they can cause severe damage to plasma-facing components. Runaway is also of interest in space and astrophysical applications, where they may be responsible for observed gamma-ray emissions.

Summary of the thesis

In this thesis, we present recent contributions to kinetic modelling of runaway in plasmas, which has been advanced by the incorporation of a full linearized Boltzmann collision model in the limit of low background temperatures. This model has been implemented into the numerical kinetic-equation solver CODE, which we have used to characterize the runaway dynamics in various scenarios. This has allowed us to assess the validity of previous collision models which have used simpler descriptions, as well as providing updated predictions for runaway generation rates. We have also demonstrated the consequences of the new model on the momentum-space distribution of runaways.

The effects of using the Boltzmann collision model is featured in Papers A, B, C and E, where it was used to describe the following processes:

Avalanche generation — In Paper A the Boltzmann operator was applied to Møller scattering, describing the elastic large-angle Coulomb

collisions between the runaway electrons and the thermal background electron population of the plasma. This generalized previous models for knock-on collisions, which were limited by approximating the momentum distribution of the runaway population, such as assuming zero pitch angle and infinite energy. We also presented a scheme to accordingly modify the Fokker-Planck operator when a large-angle collision operator is added to the kinetic equation, in order to avoid double counting of collisions. It was shown that in spite of the issues of previous models, they are mostly sufficient to predict the production rate of runaway electrons through the avalanche mechanism, with errors in the range of 10% or smaller.

Bremsstrahlung energy loss — In Paper B we applied the large-angle collision model to describe the effect of bremsstrahlung emission of the runaway dynamics for optically thin plasmas, where emitted photons are rarely absorbed by runaways. Since the average energy of the emitted photons, $m_e c^2 \langle (\gamma - \gamma_1)^2 \rangle / \langle \gamma - \gamma_1 \rangle$, is of the order of the incident electron energy $m_e c^2 \gamma$ for runaways in the 10-100 MeV range, a Fokker-Planck description is inadequate. Instead, we demonstrate that a Boltzmann operator needs to be used if one wishes to understand the momentum-space dynamics of runaways when bremsstrahlung losses are important. We showed that a significant fraction of runaways can reach twice the maximum energy predicted in a Fokker-Planck description.

Pair production during runaway — In Paper C the large-angle collision model is used to describe the momentum-space distribution of the positrons which are generated when runaway electrons interact with the thermal background plasma. An essential feature that is captured with our model is how a created positron typically co-moves with the runaway electron responsible for its creation; since the electrons are moving antiparallel to the electric field, this means that newly created positrons are moving with high speed in the direction opposite to their acceleration in the electric field. A careful analysis of the momentum-space dynamics is carried out in order to predict the fraction of created positrons that become runaway accelerated.

Collisions with a partially ionized medium — Paper E describes the theory of a Fokker-Planck equation appropriate for describing collisions with partially ionized ions. The degree to which the cloud of bound

electrons will screen out the nuclear charge is sensitive to the scattering angle; generally larger scattering angles result in a stronger enhancement of the scattering rate in comparison to the completely screened situation. For this reason, we investigated to what degree a Boltzmann model of the ion collisions would differ to the Fokker-Planck model. It was found that, although some difference was observed in the momentum-space distribution of the fast runaway population, their rate of generation was captured with high accuracy within the Fokker-Planck approximation. Paper E, which presents the details of the derivation of the new electron-ion collision model as well as further exploring its consequences on the runaway dynamics, was preceded by Papers O and R which contained its first presentation, as well as a study of the threshold electric field for avalanche multiplication in a partially ionized medium.

Papers D and F are not directly concerned with the effect of large-angle collisions, but have advanced the understanding of runaway in the following ways:

Ion runaway — We provide new insights into the runaway acceleration of *ions* in Paper D by, for the first time, considering full numerical solutions of the 2D ion kinetic equation in runaway scenarios, allowing us to study their generation and momentum-space dynamics. An important finding is that in post-disruption tokamak plasmas – where electron runaway may become a huge issue due to the numbers in which they can be generated – we demonstrate that ion runaway generation (where the tail of a thermal Mawellian population is accelerated) is unlikely to occur to any significant degree. An exception may be in the presence of a fast ion population existing before the disruption, for example injected for heating purposes or energetic helium nuclei created in fusion reactions, where they may be briefly sustained in the strong electric field due to their relatively lower collisionality. The numerical tool we developed for the study, CODION, is open source and freely available on Github [102].

Radiation synthetic diagnostics — In the final study included in the thesis, Paper F, we present a synthetic diagnostic for runaways, SOFT. The tool predicts the emission (to which the plasma is assumed to be optically thin) which would reach the aperture of a detector due to a three-dimensional runaway-electron distribution in tokamaks, which may depend arbitrarily on radius, energy and pitch angle. The tool

was originally created for predicting camera images of the synchrotron radiation emitted by a runaway beam, but has been generalized to also predict spectrometer measurements as well as those of bremsstrahlung diagnostics. The tool, which was presented in Paper F, has produced follow-up studies in Papers P, Q and S, where it was applied to model synchrotron diagnostics during runaway discharges in the Alcator C-Mod and DIII-D tokamaks. In Paper P it was also used to model the Gamma Ray Imager bremsstrahlung diagnostic at DIII-D.

Outlook

In this thesis we present recent advancements to the modelling of collisional and radiative effects on runaways. A natural framework to quantify these processes has been to consider a slab plasma, which is the simplest system exhibiting the richness of the collisional dynamics which non-locally couples the energies and pitch angles of the runaways. Since the time of the first publication in this thesis – Paper D, carried out during 2014 – our understanding of the momentum-space dynamics of runaway electrons has significantly matured. We have developed a more confident view of which collisional and radiative processes affect the runaway dynamics, some of which were obtained through the studies presented in this thesis.

However, in comparing present-day models with experimental observations of runaways in tokamaks, it is clear that the predictive capabilities of the pure momentum-space description is often limited. This demonstrates a need to extend the model to describe also spatially varying plasmas, uniting it with the momentum space effects which the work included in this thesis has mainly focused on.

In tokamaks, three spatial effects in particular directly influence the momentum-space dynamics:

(*i*) Radial transport of runaways, for example due to fluctuations of the magnetic field, where the effective rate of transport tends to be sensitive to the runaway momentum.

(*ii*) Instabilities of the plasma may affect the runaways through a wave-particle interaction, which for example will tend to flatten out inverted energy gradients in a distribution. Such bump-on-tail distributions are predicted to be produced by radiation losses, as illustrated in Papers B, H and K. The anisotropy of the runaway

distribution is also known to be a potential drive of wave instabilies.

(*iii*) The magnetic-mirror force acting on particles moving through an inhomogeneous magnetic field. This effect causes, among other things, particles of a sufficiently large pitch-angle to be trapped on the low-field side of a tokamak, where the orbit-averaged effect of the electric field is significantly reduced. This can be important for the rate of avalanche generation, since secondary electrons tend to have large pitch angles [104].

In addition, there are spatial effects which need to be accounted for that only indirectly influence the dynamics, but which may be no less important:

(*iv*) Disruption dynamics must be better understood, since the macroscopic evolution of the magnetic topology during the early stages of the disruption sets the possibility for a runaway seed to form. The destructive potential of the final runaway beam is highly sensitive to the seed; with no seed generation one may avoid the formation of a runaway beam altogether.

(*v*) The ablation of pellets and transport of impurities in cold post-disruption plasmas are essential in order to understand the distribution of the high-Z ions of the plasma. This sets the generation and dissipation rates of runaways during disruption mitigation by massive material injection, which is the system currently planned for ITER [36].

(*vi*) The self-consistent evolution of the electric field in the post-disruption plasma, which will set the runaway generation rate, but which in turn will also depend on the evolution of the runaway current profile.

These are six examples of significant gaps in present modelling and understanding, where I expect that advancements can help us bridge the gap between interpretitive and predictive modelling. In particular points (*i*-*iii*) have seen significant progress in recent years [105, 106, 107, 108], and there are ongoing efforts in the direction of the last three points. The worldwide effort in runaway modelling will certainly lead to exciting developments in the coming years.

Bibliography

[1] R. D. Gill. *Generation and loss of runaway electrons following disruptions in JET*. Nucl. Fusion **33**, 1613 (1993).

[2] A. V. Gurevich and K. P. Zybin. *Runaway breakdown and electric discharges in thunderstorms*. Phys. Usp. **44**, 1119 (2001).

[3] G. D. Holman. *Acceleration of Runaway Electrons and Joule Heating in Solar Flares*, edited by M. R. Kundu. Springer Netherlands, Dordrecht (1985).

[4] C. T. R. Wilson. *The electric field of a thundercloud and some of its effects*. Proc. Phys. Soc. London **37**, 32D (1924).

[5] C. T. R. Wilson. *The Acceleration of β-particles in Strong Electric Fields such as those of Thunderclouds*. Math. Proc. Camb. Phil. Soc. **22**, 534 (1925).

[6] A. S. Eddington. *The Internal Constitution of Stars*, Cambridge University Press, Cambridge (1926).

[7] E. R. Harrison . *Runaway and suprathermal particles*, J. Nucl. Energy, Part C Plasma Phys. **1**, 105 (1960)

[8] H. Dreicer. *Electron and ion runaway in a fully ionized gas*. Phys. Rev. **115**, 238 (1959).

[9] B. A. Trubnikov. *Particle interactions in a fully ionized plasma*, in *Reviews of Plasma Physics 1*, edited by M. A. Leontovich. Consultants Bureau Enterprises, New York (1965).

[10] M. D. Kruskal and I. B. Bernstein. *Runaway electrons in an ideal Lorentz plasma*. Phys. Fluids **7**, 407 (1964).

[11] J. W. Connor and R. J. Hastie. *Relativistic limitations on runaway electrons*. Nucl. Fusion **15**, 415 (1975).

[12] I. U. A. Sokolov. *"Multiplication" of accelerated electrons in a tokamak*. JETP Lett. **29**, 218 (1979).

[13] M. N. Rosenbluth and S. V. Putvinski. *Theory for avalanche of runaway electrons in tokamaks*. Nucl. Fusion **37**, 1355 (1997).

[14] R. Jayakumar, H. H. Fleischmann and S. J. Zweben. *Collisional avalanche exponentiation of runaway electrons in electrified plasmas*, Phys. Lett. A, **172**, 447 (1993)

[15] T. C. Hender *et al. Progress in the ITER physics basis*, Chapter 3: MHD stability, operational limits and disruptions. Nucl. Fusion **47**, 6 (2007).

[16] A. H. Boozer. *Pivotal issues on relativistic electrons in ITER*. Nucl. Fusion **58**, 036006 (2018).

[17] J. Freidberg. *Plasma Physics and Fusion Energy*. Cambridge University Press, New York (2007).

[18] J. Wesson. *Tokamaks*. Oxford University Press Inc., New York (2011).

[19] F. C. Schüller. *Disruptions in tokamaks*. Plasma Phys. Control. Fusion **31**, A135-A162 (1995).

[20] A. H. Boozer. *Theory of tokamak disruptions*. Phys. Plasmas **19**, 058101 (2012).

[21] A. Gibson. *Possibility of ion runaway in Zeta*. Nature **183**, 4654 (1959).

[22] R. W. Harvey, V. S. Chan, S. C. Chiu, T. E. Evans, M. N. Rosenbluth and D.G. Whyte. *Runaway electron production in DIII-D killer pellet experiments, calculated with the CQL3D/KPRAD model*. Phys. Plasmas **7**, 4590 (2000).

[23] P. Helander, H. Smith, T. Fülöp and L.-G. Eriksson. *Electron kinetics in a cooling plasma*. Phys. Plasmas **11**, 5704 (2004).

[24] H. Smith, P. Helander, L.-G. Eriksson and T. Fülöp. *Runaway electron generation in a cooling plasma.* Phys. Plasmas **12**, 122505 (2005).

[25] H. M. Smith, T. Fehér, T. Fülöp, K. Gál and E. Verwichte. *Runaway electron generation in tokamak disruptions.* Plasma Phys. Control. Fusion **51**, 12 (2009).

[26] P. Aleynikov and B. N. Breizman. *Generation of runaway electrons during the thermal quench in tokamaks.* Nucl. Fusion **57**, 046009 (2017).

[27] JET, EUROfusion. `https://www.euro-fusion.org/jet/`

[28] F. Romanelli and JET EFDA Contributors. *Overview of the JET results with the ITER-like wall.* Nucl. Fusion **53**, 104002 (2013).

[29] ITER organization. `http://www.iter.org/`

[30] E. M. Hollmann *et al. Status of research toward the ITER disruption mitigation system.* Phys. Plasmas **22**, 021802 (2015).

[31] A. H. Boozer. *Theory of runaway electrons in ITER: Equations, important parameters, and implications for mitigation.* Phys. Plasmas **22**, 032504 (2015).

[32] M. Lehnen *et al. Impact and mitigation of disruptions with the ITER-like wall in JET.* Nucl. Fusion **53**, 093007 (2013).

[33] P. Helander, L-G. Eriksson and F. Andersson. *Runaway acceleration during magnetic reconnection in tokamaks.* Plasma Phys. Control. Fusion **44**, 12B (2002).

[34] J. R. Martín-Solís, A. Loarte and M. Lehnen. *Formation and termination of runaway beams in ITER disruptions.* Nucl. Fusion **57**, 066025 (2017).

[35] B. N. Breizman. *Marginal stability model for the decay of runaway electron current.* Nucl. Fusion **54**, 072002 (2014).

[36] M. Lehnen *et al. Disruptions in ITER and strategies for their control and mitigation.* J. Nucl. Mater. **463**, 39 (2015).

[37] H. P. Furth and P. H. Rutherford. *Ion runaway in tokamak discharges.* Phys. Rev. Lett. **28**, 545 (1972).

[38] P. Helander, L.-G. Eriksson, R. J. Akers, C. Byrom, C. G. Gimblett and M. R. Tournianski. *Ion acceleration during reconnection in MAST*. Phys. Rev. Lett. **89**, 235002 (2002).

[39] T. Fülöp, and S. Newton. *Alfvénic instabilities driven by runaways in fusion plasmas*. Phys. Plasmas **21**, 080702 (2014).

[40] A. Sykes, the START Team, the NBI Team, the MAST Team and the Theory Team. *The spherical tokamak programme at Culham*. Nucl. Fusion **39**, 1271 (1999).

[41] MAST, CCFE. `http://www.ccfe.ac.uk/mast.aspx`

[42] G. D. Holman. *DC electric field acceleration of ions in solar flares*. Astrophys. J. **452**, 451 (1995).

[43] S. Eilerman, J. K. Anderson, J. S. Sarff, C. B. Forest, J. A. Reusch, M. D. Nornberg and J. Kim. *Runaway of energetic test ions in a toroidal plasma*. Phys. Plasmas **22**, 020702 (2015).

[44] J. K. Anderson, J. Kim, P. J. Bonofiglo, W. Capecchi, S. Eilerman, M. D. Nornberg, J. S. Sarff and S. H. Sears. *Dynamics of reconnection-driven runaway ion tail in a reversed field pinch plasma*. Phys. Plasmas **23**, 055702 (2016).

[45] A. A. Vlasov. *The vibrational properties of an electron gas*. Sov. Phys. Usp. **10**, 721 (1968).

[46] R. D. Hazeltine and J. D. Meiss. *Plasma Confinement*. Dover Publications, New York (2003).

[47] N. N. Bogolyubov. *Problems of a Dynamical Theory in Statistical Physics*. State Technical Press, Moscow, 1946. English translation available in *Studies in Statistical Mechanics*, vol. 1 by J. de Boer and G. E. Uhlenbeck, North Holland Publishing Company, Amsterdam (1962).

[48] M. Born and H. S. Green. *A General Kinetic Theory of Liquids*. Cambridge University Press, London (1949).

[49] H. S. Green. *The Molecular Theory of Fluids*. Interscience Publishers, Inc., New York (1952).

[50] J. G. Kirkwood. *The statistical mechanical theory of transport processes I & II.* J. Chem. Phys. **14**, 180 (1946); **15**, 72 (1947).

[51] J. Yvon. *La thèorie des fluides et l'équation d'état: actualitès scientifiques et industrielles.* Hermann & Cie, Paris (1935).

[52] J. Liouville. *Note sur la Théorie de la Variation des constantes arbitraires.* J. Math. App. **3**, 342 (1838).

[53] H. Goldstein, C. Poole and J. Safko. *Classical Mechanics*, third edition. Addison Wesley, San Francisco (2002).

[54] E. A. Frieman. *On a new method in the theory of irreversible processes.* J. Math. Phys **4**, 410 (1963).

[55] G. Sandri. *The foundations of nonequilibrium statistical mechanics, I & II.* Ann. Phys. **24**, 332 (1963).

[56] D. C. Montgomery and D. A. Tidman. *Plasma kinetic theory*, McGraw-Hill, Inc., New York (1964).

[57] G. Ecker. *Theory of Fully Ionized Plasmas.* Academic Press, Inc., New York (1972).

[58] L. Landau. *The transport equation in the case of Coulomb interactions.* Phys. Z. Sowjet **10**, 154 (1936).

[59] L. Boltzmann. *Weitere Studien über das Wärmegleichgewicht unter Gasmoleculen.* Wien Ber. **66**, 275 (1872). Translation in English can be found in L. Boltzmann, *Further studies on the thermal equilibrium of gas molecules*, in *The Kinetic Theory of Gases: An anthology of classic papers with historical commentary* by S. G. Brush. Imperial College Press, London (2003).

[60] L. Boltzmann. *Vorlesungen uber Gastheorie.* J. A. Barth, Leipzig (1896).

[61] C. Cercignani and G. M. Kremer. *The Relativistic Boltzmann Equation: Theory and Applications.* Birkhäuser Verlag Basel, Berlin (2002).

[62] W. Heitler. *The Quantum Theory of Radiation.* Oxford University Press, London (1954).

[63] S. Weinberg. *The Quantum Theory of Fields, Volume 1: Foundations.* Cambridge University Press, Cambridge (2005).

[64] C. Cercignani. *Theory and Application of the Boltzmann Equation.* Scottish Academic Press, Edinburgh (1975).

[65] A. D. Fokker. *Die mittlere Energie rotierender elektrischer Dipole im Strahlungsfeld.* Annalen der Physik **348**, 810 (1914).

[66] M. Planck. *Über einen Satz der Statistischen Dynamik und seine Erweiterung in der Quantentheorie.* S. B. K. Preuss. Akad. Wiss. Berlin **N**, 324 (1917).

[67] S. T. Beliaev and G. I. Budker. *The relativistic kinetic equation.* Sov. Phys. Dokl. **1**, 218 (1956).

[68] H. Akama. *Relativistic Boltzmann equation for plasmas.* J. Phys. Soc. Japan **28**, 478 (1970).

[69] E. M. Lifshitz and L. P. Pitaevskii. *Physical Kinetics*, Volume 10 in *Course of Theoretical Physics.* Butterworth-Heinemann, Oxford (1981).

[70] P. Helander and D. J. Sigmar. *Collisional Transport in Magnetized Plasmas.* Cambridge University Press, New York (2002).

[71] H. Bethe. *Zur theorie des durchgangs schneller korpuskularstrahlen durch materie.* Annalen der Physik **397**, 325 (1930).

[72] S. P. Sauer, J. Oddershede, J. R. Sabin. *Chapter three - the mean excitation energy of atomic ions* Concepts of Mathematical Physics in Chemistry: A Tribute to Frank E. Harris - Part A, Advances in Quantum Chemistry, **71**, 29. Academic Press (2015).

[73] N. F. Mott and H. S. W. Massey. *The Theory of Atomic Collisions.* Clarendon Press, Oxford (1965).

[74] A. Gulans, S. Kontur, C. Meisenbichler, D. Nabok, P. Pavone, S. Rigamonti, S. Sagmeister, U. Werner and C. Draxl. EXCITING*: a full-potential all-electron package implementing density-functional theory and many-body perturbation theory.* Journal of Physics: Condensed Matter **26**, 363202 (2014).

[75] M. J. Frisch *et al. Gaussian 16 Revision B.01.* Gaussian Inc. Wallington CT (2016).

[76] G. Papp, M. Drevlak, T. Fülöp and P. Helander. *Runaway electron drift orbits in magnetostatic perturbed fields.* Nucl. Fusion **51**, 043004 (2011).

[77] M. N. Rosenbluth, W. M. MacDonald and D. L. Judd. *Fokker-Planck equation for an inverse-square force.* Phys. Rev. **107**, 1 (1957).

[78] M. Landreman, A. Stahl and T. Fülöp. *Numerical calculation of the runaway electron distribution function and associated synchrotron emission.* Comp. Phys. Comm. **185**, 847 (2014).

[79] J. Larmor. *On the theory of the magnetic influence on spectra; and on the radiation from moving ions.* Philos. Mag. Series 5 **44**, 503 (1897).

[80] M. Abraham. *Prinzipien der Dynamik des Elektrons.* Ann. Phys. **315**, 105 (1902).

[81] P. A. M. Dirac. *Classical theory of radiating electrons.* Proc. R. Soc. A **167**, 148 (1938).

[82] F. Andersson, P. Helander and L.-G. Eriksson. *Damping of relativistic electron beams by synchrotron radiation.* Phys. Plasmas **8**, 5221 (2001).

[83] J. D. Jackson. *Classical Electrodynamics.* John Wiley & Sons, Inc., Hoboken (1999).

[84] I. H. Hutchinson. *Principles of Plasma Diagnostics.* Cambridge University Press, New York (2002).

[85] G. Racah. *Sopra L'irradiazione nell'urto di particelle veloci.* Il Nuovo Cimento **11**, 461 (1934).

[86] P. T. McCormick, D. G. Keiffer and G. Parzen. *Energy and angle distribution of electrons in bremsstrahlung.* Phys. Rev. **103**, 29 (1956).

[87] I. Fernández-Gómez, J. R. Martín-Solís and R. Sánchez. *Determination of the parametric region in which runaway electron energy losses are dominated by bremsstrahlung radiation in tokamaks.* Phys. Plasmas **14**, 072503 (2007).

[88] M. Bakhtiari, G. J. Kramer, M. Takechi, H. Tamai, Y. Miura, Y. Kusama and Y. Kamada. *Role of Bremsstrahlung Radiation in Limiting the Energy of Runaway Electrons in Tokamaks.* Phys. Rev. Lett. **94**, 215003 (2005).

[89] M. Bakhtiari, G. J. Kramer and D. G. Whyte. *Momentum-space study of the effect of bremsstrahlung radiation on the energy of runaway electrons in tokamaks.* Phys. Plasmas **12**, 102503 (2005).

[90] C. Paz-Soldan, C. M. Cooper, P. Aleynikov, D. C. Pace, N. W. Eidietis, D. P. Brennan, R. S. Granetz, E. M. Hollmann, C. Liu, A. Lvovskiy, R. A. Moyer and D. Shiraki. *Spatiotemporal Evolution of Runaway Electron Momentum Distributions in Tokamaks.* Phys. Rev. Lett **118**, 255002 (2017).

[91] C. Paz-Soldan, C. M. Cooper, P. Aleynikov, N. W. Eidietis, A. Lvovskiy, D. C. Pace, D. P. Brennan, E. M. Hollmann, C. Liu, R. A. Moyer and D. Shiraki. *Resolving runaway electron distributions in space, time, and energy.* Phys. Plasmas **25**, 056105 (2018).

[92] E. M. Hollmann, P. B. Parks, N. Commaux, N. W. Eidietis, R. A. Moyer, D. Shiraki, M. E. Austin, C. J. Lasnier, C. Paz-Soldan and D. L. Rudakov. *Measurement of runaway electron energy distribution function during high-Z gas injection into runaway electron plateaus in DIII-D.* Phys. Plasmas **22**, 056108 (2015).

[93] R. J. Zhou, I. M. Pankratov, L. Q. Hu, M. Xu and J. H. Yang. *Synchrotron radiation spectra and synchrotron radiation spot shape of runaway electrons in Experimental Advanced Superconducting Tokamak.* Physics of Plasmas **21**, 063302 (2014).

[94] G. R. Blumenthal and R. J. Gould. *Bremsstrahlung, synchrotron radiation, and Compton scattering of high-energy electrons traversing dilute gases.* Rev. Mod. Phys. **42**, 237 (1970).

[95] I. M. Pankratov. *Analysis of the Synchrotron Radiation Emitted by Runaway Electrons.* Plasma Physics Reports **22**, 535 (1996).

[96] A. Stahl, M. Landreman, G. Papp, E. Hollmann and T. Fülöp. *Synchrotron radiation from a runaway electron distribution in tokamaks*. Phys. Plasmas **20**, 093302 (2013).

[97] P. Helander and D. J. Ward. *Positron Creation and Annihilation in Tokamak Plasmas with Runaway Electrons*. Phys. Rev. Lett. **90**, 135004 (2003).

[98] J. Alwall *et al. The automated computation of tree-level and next-to-leading order differential cross sections, and their matching to parton shower simulations.* Journal of High Energy Physics **7**, 79 (2014).

[99] D. A. Gryaznykh. *Cross Section for the Production of Electron-Positron Pairs by Electrons in the Field of a Nucleus*. Phys. Atom. Nuclei **61**, 394 (1998).

[100] V. M. Budnev, I. F. Ginzburg, G. V. Meledin and V. G. Serbo. *The two-photon particle production mechanism. Physical problems. Applications. Equivalent photon approximation*. Phys. Reports **15**, 181 (1975).

[101] Y. Guanying, J. Liu, J. Xie and J. Li. *Detection of tokamak plasma positrons using annihilation photons*. Fusion Eng. Design **118**, 124 (2017).

[102] CODION is an open-source tool, available for download on GitHub. `http://github.com/Embreus/CODION`

[103] F. L. Hinton. *Collisional Transport in Plasma*, in *Basic Plasma Physics I*, edited by A. A. Galeev and R. N. Sudan. North-Holland Publishing Company, Amsterdam (1983).

[104] E. Nilsson, J. Decker, N. J. Fisch and Y. Peysson. *Trapped-electron runaway effect*. J. Plasma Phys. **81**, 475810403 (2015).

[105] T. Hauff and F. Jenko. *Runaway electron transport via tokamak microturbulence*. Phys. Plasmas **16**, 102308 (2009).

[106] G. Papp, M. Drevlak, T. Fülöp, P. Helander and G. I. Pokol. *Runaway electron losses caused by resonant magnetic perturbations in ITER*. Plasma Phys. Control Fusion **53**, 095004 (2011).

[107] C. Liu, L. Shi, E. Hirvijoki, D. P. Brennan, A. Bhattacharjee, C. Paz-Soldan and M. E. Austin. *The effects of kinetic instabilities on the electron cyclotron emission from runaway electrons.* Nucl. Fusion **58**, 096030 (2018).

[108] C. Liu, H. Qin, E. Hirvijoki, Y. Wang and J. Liu. *Conservative magnetic moment of runaway electrons and collisionless pitch-angle scattering.* Nucl. Fusion **58**, 106018 (2018).